

RESEARCH ARTICLE

Published  
2022-11-02

Cite as

Mohammad Javad Razmjooei  
and Nicolas Thibault (2022)  
*Morphometric changes in two  
Late Cretaceous calcareous  
nannofossil lineages support  
diversification fueled by  
long-term climate change*, Peer  
Community Journal, 2: e64.


Correspondence  
[nt@ign.ku.dk](mailto:nt@ign.ku.dk)

Peer-review  
Peer reviewed and  
recommended by  
PCI Paleontology,  
<https://doi.org/10.24072/pci.paleo.100011>



This article is licensed  
under the Creative Commons  
Attribution 4.0 License.

## Morphometric changes in two Late Cretaceous calcareous nannofossil lineages support diversification fueled by long-term climate change

Mohammad Javad Razmjooei <sup>1,2</sup> and Nicolas  
Thibault <sup>1</sup>

Volume 2 (2022), article e64

<https://doi.org/10.24072/pcjournal.183>

### Abstract

Morphometric changes have been investigated in the two groups of calcareous nannofossils, *Cribrosphaerella ehrenbergii* and *Microrhabdulus undosus* across the Campanian to Maastrichtian of the Zagros Basin of Iran. Results reveal a common episode of size increase at c. 76 Ma, with a sudden increase in the size of *C. ehrenbergii* and with the emergence of a newly defined, larger species *Microrhabdulus zagrosensis* n.sp. An even larger species emerges at c. 69 Ma within the *Microrhabdulus* lineage, *Microrhabdulus sinuosus* n.sp. The timing of these size changes and origination events matches global changes in nannoplankton diversity and/or in diversity of other planktonic organisms and marine invertebrates. Comparison with long-term global climate change supports that these two distinct episodes of morphological change coincide respectively with the late Campanian carbon isotope event and acceleration of cooling and with climatic instability across the mid-Maastrichtian event.

<sup>1</sup>Department of Geosciences and Natural Resource Management, University of Copenhagen – Copenhagen, Denmark, <sup>2</sup>Department of Geological Sciences, Stockholm University – Stockholm, Sweden



## 1. Introduction

Extant and fossil calcareous microplankton commonly comprise numerous cryptic and/or pseudo-cryptic species (Sáez et al., 2003; de Vargas et al., 2004). Morphometric measurements such as size variation are regularly conducted on calcareous nannofossils in order to assess changes in morphology that often lead to the erection of new species and lineages (Bollmann, 1997; Geisen et al., 2004; Shamrock & Watkins, 2009). Among planktonic microfossils, the fossil record of calcareous nannoplankton is particularly important as it is intimately linked to the carbon cycle, global changes in climate, and oceanography. Morphological changes in calcareous nannofossils have been the subject of numerous studies across their evolutionary history in the Meso-Cenozoic. Perhaps due to better preserved records, Cenozoic biometric studies are abundant, while Mesozoic studies have focused mostly on specific intervals such as the Early to Middle Jurassic (Suchéras-Marx et al., 2010; Suan et al., 2010; Peti & Thibault, 2017; Peti et al., 2021; Menini et al., 2021; Faucher et al., 2022; López-Otálvaro et al., 2012; Ferreira et al., 2017) or Early to mid-Cretaceous (Bornemann & Mutterlose, 2006; Barbarin et al., 2012; Lübke & Mutterlose, 2016; Bottini & Faucher, 2020; Wulff et al., 2020). In comparison to the latter periods, and considering that the Santonian to Maastrichtian interval bears the highest diversity within the overall evolutionary history of calcareous nannoplankton (Bown et al. 2004), this significant part of the Late Cretaceous has been the subject of relatively few biometric studies mostly focused on Arkhangelskiellaceae and the *Eiffelithus* lineages (Girgis, 1987; Faris 1995; Thibault et al., 2004; Linnert & Mutterlose, 2009; Shamrock & Watkins, 2009; Thibault, 2010; Linnert et al., 2014). Such studies are of fundamental importance in taxonomy, often revealing the presence of pseudo-cryptic taxa (Shamrock & Watkins, 2009; Suchéras-Marx et al., 2010; Thibault, 2010; Peti & Thibault, 2017; Peti et al., 2021), but also revealing trends that coincide with paleoenvironmental change (Suan et al., 2010; Ferreira et al., 2017; Lübke & Mutterlose, 2016; Bottini & Faucher, 2020; Wulff et al., 2020). During the investigation of samples from the Shahneshin section (Zagros basin, Iran, Razmjooei et al., 2018; Fig. 1), we noticed interesting patterns in size and morphology of *Cribrosphaerella ehrenbergii* and *Microrhabdulus undosus*, two species that are frequent to common in Santonian to Maastrichtian low-latitude assemblages. The paleoecology of *M. undosus* is unclear, and it is essentially a cosmopolitan taxon (Lees, 2002). Although *C. ehrenbergii* is also a cosmopolitan taxon (Thierstein, 1981; Henriksson & Malmgren, 1997; Lees, 2002), several authors have considered this species as having a greater affinity toward cool sea-surface temperatures (Wise, 1983; Pospichal & Wise, 1990; Watkins, 1992; Ovechkina & Alekseev, 2002, 2005; Razmjooei et al., 2020b), possibly enhanced in more proximal conditions (Razmjooei et al., 2020b), while others postulated a controversial affinity to nutrient availability. For instance, Erba et al. (1995) suggested that blooms of *C. ehrenbergii* could indicate increased surface water productivity, while Linnert et al. (2011) inferred a lower nutrient affinity for this species. The purpose of this study is to better constrain *Cribrosphaerella* and *Microrhabdulus* taxonomies, investigate biometric changes in these two lineages, and evaluate the timing of these changes relative to global changes in temperature and the carbon cycle.

## 2. Geological setting and a summary of earlier works

The Upper Cretaceous pelagic deposits of the Gurpi Fm. in the Shahneshin section consist of regular carbonate cycles of dark- to pale-gray marl and dark-gray to light-yellow argillaceous limestones with a number of resistant carbonate beds forming ridges in the landscape that constitute excellent markers across the field area. The section possesses the advantage of bearing a detailed and precise stratigraphic framework of calcareous nannofossils, planktonic foraminifera, marine palynomorphs, and bulk carbonate carbon isotopes (Razmjooei et al., 2018; Fig. 2). The Shahneshin section is situated in the central part of the Zagros folded zone, west of Fars province, on the northeast of Kazerun city and the northwest of the Shahneshin anticline, with geological coordinates of N29° 44' 47''; E51° 46' 31'' for the base of the section, and N29° 44' 40.69''; E51° 46' 26.87'', for the top of the Cretaceous sequence (Fig. 1).

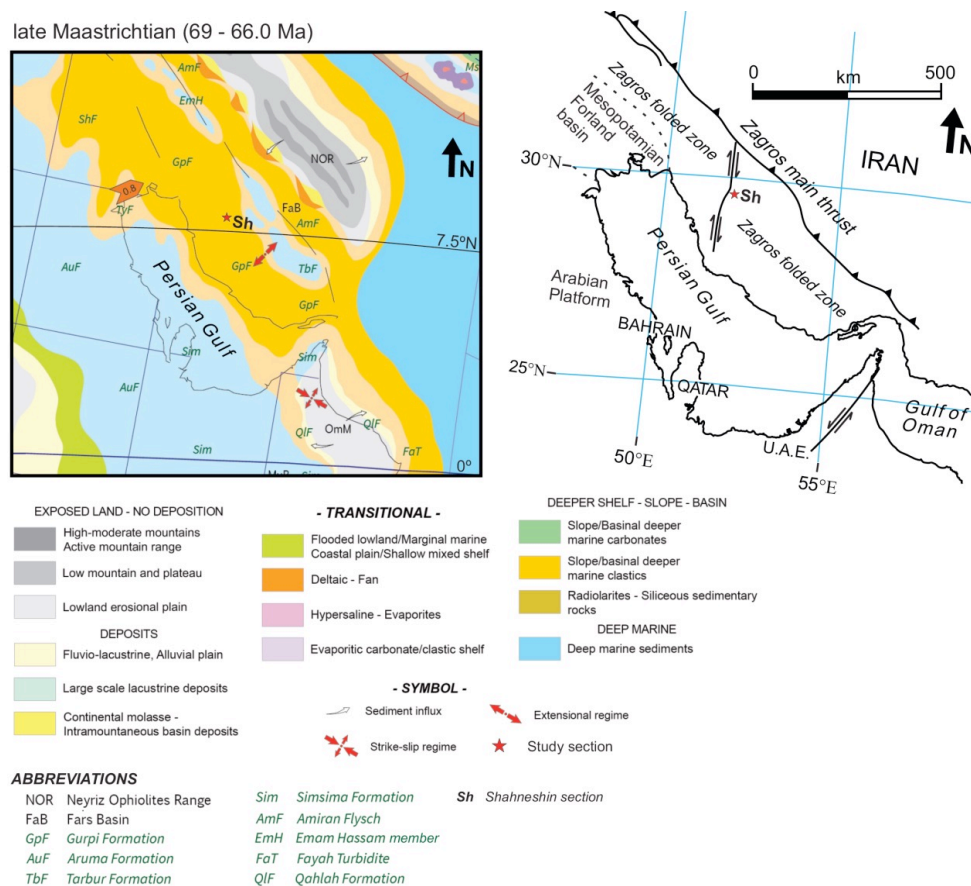


**Figure 1.** A) Paleogeography of the Maastrichtian with the position of the Zagros Basin (Barrier et al., 2018). B) Recent geological map of the Zagros Basin and the location of the studied area.

The first stratigraphic framework on Shahneshtin was carried out in 2014 based on integrated calcareous nannofossil biostratigraphy and carbon isotope stratigraphy (Razmjooei et al., 2014). In 2018, the detailed integrated bio- (calcareous nannofossils, planktonic foraminifera and marine dinoflagellate cysts) and stable carbon isotope stratigraphy, with a subsequent graphic correlation to Tethyan reference sections (Gubbio, Italy) led to proposing an age model for the Gurpi succession and for numerous Late Cretaceous planktonic foraminifera and calcareous nannofossil bioevents (Razmjooei et al., 2018) (Fig. 2). According to these two earlier works, two significant hiatuses were recorded in the latest Campanian and/or across the Campanian-Maastrichtian boundary and across the topmost Maastrichtian to early Danian. Later on, combined with facies change, carbonate content and changes in absolute abundance of calcareous nannofossils, a sequence stratigraphic interpretation was proposed for the Gurpi Fm. at Shahneshtin (Razmjooei et al., 2020a). Moreover, detailed abundance counts and statistical analysis were investigated on the calcareous nannofossil assemblage to explore its response to Late Cretaceous climatic changes. According to this study, a Late Cretaceous intensification of cooling across the late Campanian-early Maastrichtian, a mid-Maastrichtian warming episode, and a late Maastrichtian cooling episode could be delineated in Zagros along with accompanying proximal/distal trends possibly influencing the nannofossil assemblage (Razmjooei et al., 2020b).

### 3. Material and methods

The calcareous nannofossil biometric analysis has been carried out on smear slides prepared by Razmjooei et al. (2018) based on the standard preparation method of Bown & Young (1998). The calcareous nannofossil zonations are based on the CC biozonation of Sissingh (1977) modified by Perch-Nielsen (1985) and the UCTP (Tethyan Province) of Burnett (1998), using the taxonomic concepts of Perch-Nielsen (1985), Young & Bown (1997) as well as Shamrock & Watkins (2009).

Due to the moderate to poor preservation of calcareous nannofossils (Razmjooei et al., 2020b), only the best-preserved samples with frequent to common abundance of the two lineages *C. ehrenbergii* and *M. undosus* in the upper Campanian-Maastrichtian were chosen for biometric measurements (Fig. 2). The length of *C. ehrenbergii* has been investigated in standard smear-slides for a total of 29 samples spanning the entire Campanian and Maastrichtian intervals of the Shahneshin section (Table 1; Supplementary Appendix 1). Because of the lower abundance, changes in the size and morphology of *M. undosus* group have been investigated in 17 samples from 170 to 342 m (upper lower Campanian to Maastrichtian), where the abundance of the species was high enough to allow for the measurement of several specimens (Supplementary Appendix 1). The sample spacing varies mostly between 7 to 9 m with time intervals varying between 250 and 900 kyr according to the age-model presented in Razmjooei et al. (2018) (Supplementary Appendices 3 and 4). When possible, we measured the length and width of up to 50 specimens of *C. ehrenbergii*. Three samples at 106.2, 123.1, and 186 m had a low abundance of this species so only 19, 25 and 40 specimens were measured in them, respectively (Table 1).

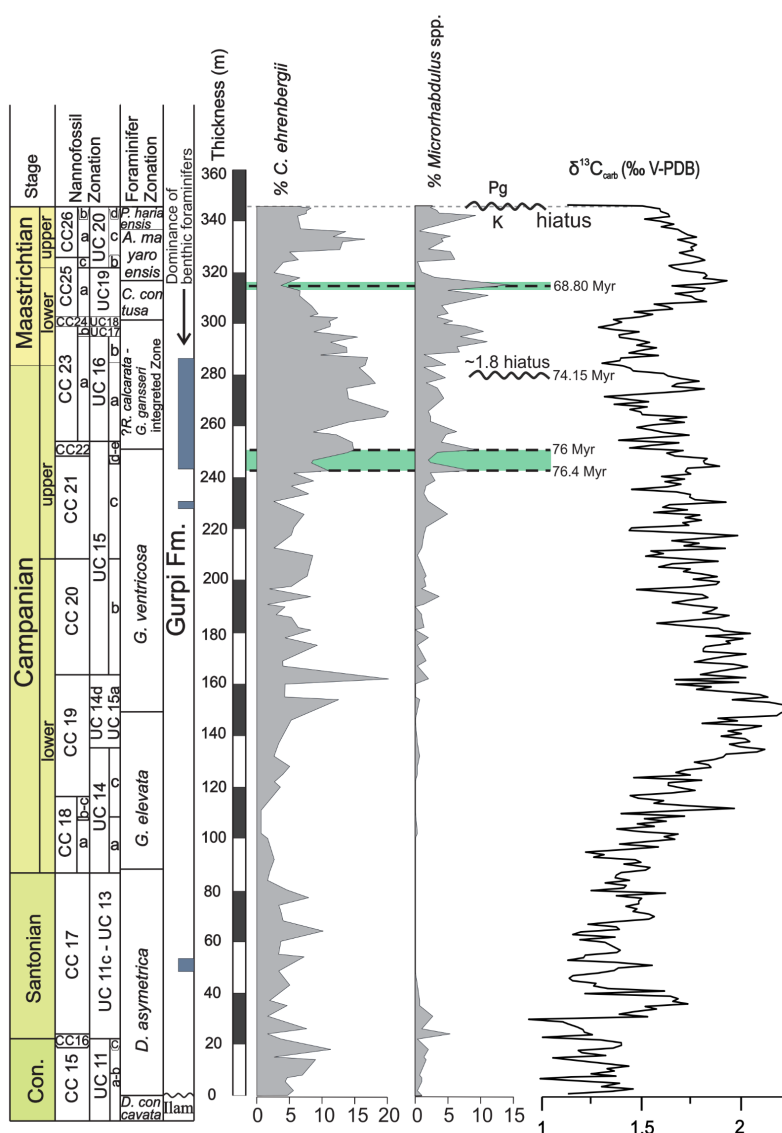


**Figure 2.** Integrated biostratigraphy and bulk carbonate carbon isotope records of the Shahneshin section based on Razmjooei et al. (2018), along with the relative abundances of *Microrhabdulus* spp. and *C. ehrenbergii* according to Razmjooei et al. (2020b). The two green areas with dashed lines indicate the two stratigraphic levels with major shifts observed in the morphology of the two taxa. Stratigraphic and isotopic data from Razmjooei et al. (2018). The given absolute ages are based on the age-model presented in Razmjooei et al. (2018).



For *M. undosus* group, we could measure the length and width of up to 30 specimens in only 8 samples. The total number of specimens measured in other samples is provided in Table 2. The biometric measurements have been performed using a light microscope (Leica DM750P) at a magnification of 1250× with a Leica DFC320 digital camera and the ImageJ 1.50i software. In total, 1385 pictures of *C. ehrenbergii* and 336 pictures of *M. undosus* were captured throughout the Campanian–Maastrichtian interval. All the images were taken under the cross-polarised light (XPL). Despite the heterogeneity of the *M. undosus* group dataset, our investigations of size changes in this group were paralleled with systematic observations on the patterns of individual laths that characterize this taxon (Supplementary Appendix 2). As described further, significant changes in the size of the *M. undosus* group occur at precise stratigraphic intervals and coincide with significant changes in lath patterns (Figs. 3 and 4). Accordingly, biometric measurements on individual samples are used to follow the progression of these patterns across the stratigraphy of the section and the statistical significance in the difference between potential morphotypes is tested via density plots using the Matlab® script of Thibault et al. (2018) and via the comparison of distribution histograms produced in PAST® (Hammer et al., 2001) for three distinct stratigraphic intervals that bear enough specimens for reliable statistics (Fig. 5).

A settling technique was adapted from Bown & Young (1998) to obtain suitable slides for Scanning Electron Microscope (SEM) analyses and eliminate particles bigger than 30 µm and smaller than 1 µm. Moreover, to have a cleaner surface for observing coccoliths and taking pictures of coccolith individuals under SEM, the suspensions from gravity settling were subjected to the filtration technique using membrane filters with 0.8 µm pore size. Finally, to observe and capture images of the same nannofossil individuals under the light and SEM microscopes, we applied the slide preparation technique proposed by Gallagher (1988) and Pirini Radrizzani et al. (1990) using a copper grid with the coordinate system.

**Table 1.** Number of measured specimens, mean length (µm), mean width (µm), standard deviation and 95% confidence intervals for each sample investigated for the size of *Cribrosphaerella ehrenbergii*.

height (m)	Age (Razmjooei et al., 2018)	N	mean length	mean width	STD length	95% STD length	STD width	95% STD width
342.0	~66.10	50	6.85	5.24	0.96	0.27	0.81	0.22
333.0	~67.00	50	6.26	4.80	1.00	0.28	0.89	0.25
315.0	~68.90	50	6.68	5.02	1.13	0.31	0.93	0.26
307.0	~69.80	50	6.48	4.92	0.70	0.19	0.61	0.17
299.0	~70.60	50	6.50	5.00	1.03	0.29	1.05	0.29
291.0	~71.40	50	6.84	5.18	0.82	0.23	0.84	0.23
283.0	~74.15	50	6.80	5.10	0.90	0.25	0.73	0.20
275.0	~74.50	50	6.46	5.01	0.78	0.22	0.74	0.20
266.0	~74.85	50	6.93	5.24	1.16	0.32	1.02	0.28
258.0	~75.20	50	6.90	5.35	1.00	0.28	0.88	0.24
250.0	~75.50	50	6.24	4.77	0.89	0.25	0.84	0.23
243.0	~75.80	50	6.42	4.99	0.80	0.22	0.73	0.20
234.0	~76.15	50	5.68	4.39	0.82	0.23	0.72	0.20
226.0	~76.50	50	6.10	4.69	0.85	0.23	0.64	0.18
218.0	~76.80	50	5.68	4.36	0.80	0.22	0.70	0.19
210.0	~77.20	50	6.41	4.99	0.64	0.18	0.52	0.14
202.0	~77.50	49	5.59	4.29	1.08	0.30	0.90	0.25
195.7	~77.75	50	5.78	4.46	1.05	0.29	0.89	0.25
186.0	~78.20	40	5.50	4.22	0.97	0.30	0.75	0.23
178.0	~78.50	47	6.02	4.68	0.75	0.21	0.65	0.18
170.0	~78.80	50	5.17	3.96	0.58	0.16	0.48	0.13
162.0	~79.20	50	5.11	3.93	0.68	0.19	0.51	0.14
154.2	~79.45	50	5.55	4.30	0.61	0.17	0.62	0.17
148.3	~79.70	50	5.71	4.44	0.72	0.20	0.73	0.20
139.2	~80.10	50	5.58	4.36	0.71	0.20	0.67	0.18
130.3	~80.45	48	6.13	4.79	0.82	0.23	0.81	0.22
123.1	~80.70	25	5.14	3.92	0.94	0.37	0.73	0.29
106.2	~82.70	19	5.39	4.21	0.64	0.28	0.61	0.27
89.7	~84.25	50	5.64	4.31	0.72	0.20	0.59	0.16

**Table 2.** Number of measured specimens, maximum length ( $\mu\text{m}$ ), mean width ( $\mu\text{m}$ ), standard deviation and 95% confidence intervals for each sample investigated for the size of *Microrhabdulus undosus* group.

height(m)	N	max length	mean width	STD width	95% STD width
342.0	30	27.40	2.48	0.31	0.11
333.0	30	20.60	2.31	0.31	0.11
315.0	30	20.00	2.07	0.25	0.09
307.0	10	15.10	2.00	0.18	0.11
299.0	15	16.70	1.93	0.24	0.12
291.0	30	17.60	1.84	0.20	0.07
283.0	20	19.40	1.95	0.18	0.08
275.0	8	15.90	1.89	0.18	0.13
258.0	32	19.30	2.03	0.22	0.08
250.0	30	19.10	1.85	0.19	0.07
243.0	30	21.10	1.46	0.13	0.05
234.0	10	15.20	1.49	0.13	0.08
226.0	30	20.40	1.63	0.08	0.03
218.0	6	17.50	1.52	0.13	0.11
210.0	3	10.80	1.50	0.20	0.23
195.7	6	19.30	1.52	0.15	0.12
178.0	7	15.40	1.46	0.05	0.04
170.0	9	16.00	1.54	0.19	0.12

## 4. Results

### 4.1. Preservation of the calcareous nannofossils

According to the previous study by Razmjooei et al. (2020b) and following the criteria proposed by Roth (1978), the preservation of calcareous nannofossils in the Shahneshtin section is moderate to poor. This moderate to poor preservation of the assemblage is expressed by the significantly high abundance of the solution-resistant species *Watznaueria barnesiae* (Roth & Krumbach, 1986) throughout the Campanian-Maastrichtian interval, as well as by the low species richness (generally <30 species) and the absence of small coccoliths such as small *Biscutum*, *Zeughradotus erectus*, or *Prediscosphaera stoveri*. The influence of preservation is also depicted in the second axis of a principal component analysis performed on the nannofossil assemblage as well as through the relative negative offset in bulk carbonate  $\delta^{18}\text{O}$  values compared to better preserved tropical sections of the same interval (Razmjooei et al., 2020b). Even though we cannot exclude that the two studied lineages, *C. ehrenbergii* and *M. undosus* group, have been affected by diagenesis, they were large enough ( $> 3 \mu\text{m}$ ) to prevent a major influence of diagenesis on size changes since mostly small coccoliths  $< 3 \mu\text{m}$  tend to be preferentially dissolved when undergoing dissolution. The preservation of the two lineages is good enough to observe the main features of their morphology, for instance, the shields with R-units and V-unit crystals of *C. ehrenbergii*. When this species is strongly dissolved, the perforations in the central area are not visible anymore and the central area is thus empty. Our specimens often exhibit perforations in the central area, and when no perforations were clearly visible, the measured specimens were complete with clear thick rims. As for *M. undosus*, it is clear that preservation has affected this species, for instance, many specimens are fragmented and therefore the total length would represent a biased criterion. SEM observations reported below show some dissolution and recrystallization features but these features do not affect the diameter of the rod which is reflected in our data by the measured width in XPL. Also, undulating laths around the central rod of *M. undosus* group specimens remain very clearly visible and morphological patterns in-between the various morphospecies evidenced in our data are well depicted in documented specimens (Fig. 4).

### 4.2. *C. ehrenbergii* relative abundance and size variations

As illustrated in figure 2, the relative abundance of *C. ehrenbergii* averages 5% in the Coniacian to Santonian interval, then reaches a minimum of less than 1% in the earliest Campanian, peaks at up to more than 12% in the upper part of Zone CC19, and remains around 5% again through CC20 and CC21. In the

latest Campanian Zone CC22, a significant increase is observed with values reaching up to 15%. An acme of the species with relative abundances higher than 10% and peaking up to maximum values of 20% is observed throughout the uppermost Campanian CC22 Zone to the lower Maastrichtian CC24 Zone. The relative abundance of *C. ehrenbergii* decreases again down to 5% in the mid-Maastrichtian and remains below 10% within CC25. The upper Maastrichtian subzones CC26a and UC20b-c<sup>TP</sup> are characterized by a second acme of the species reaching values as high as 17%. A slight decrease of the species is observed in the uppermost Maastrichtian samples from CC26a and UC20c<sup>TP</sup> to the Cretaceous-Paleogene (K-Pg) boundary (Fig. 2). From our biometric measurements, it appears that the size of *C. ehrenbergii* remains essentially stable around a mean length of 5.5  $\mu\text{m}$  throughout the lower Campanian to upper Campanian Zone CC21. A significant increase in the average size of *C. ehrenbergii* occurs in coincidence with the onset of the first acme of the species within upper Campanian Zone CC22. Thereafter, the size of *C. ehrenbergii* remains stable around a mean of 6.5  $\mu\text{m}$  in the remaining upper Campanian to Maastrichtian (Fig. 3). Comparison of two distribution histograms for stratigraphic intervals below and above 240 m highlights the near complete disappearance of *C. ehrenbergii* representatives smaller than 5  $\mu\text{m}$  and appearance of giant specimens > 8  $\mu\text{m}$  in upper Campanian to Maastrichtian zones CC22 to CC26 (Fig. 5, distribution histograms A and B).

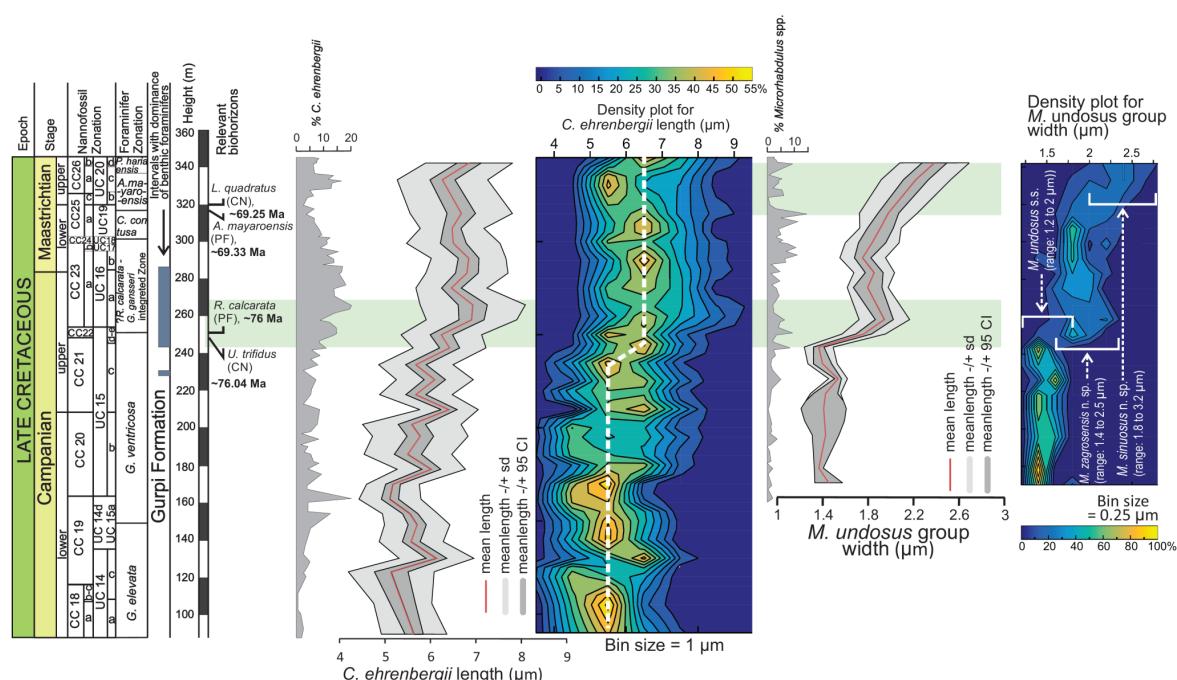


**Figure 3.** Mean length ( $\mu\text{m}$ ) of *C. ehrenbergii* and mean width ( $\mu\text{m}$ ) of the *Microrhabdulus undosus* group along with their standard deviation and 95% confidence interval envelopes. Density plots for both groups provide the percentage of data for each size bin. The two green areas indicate the stratigraphic levels where major shifts in morphology are observed. Relevant nannofossil and foraminifera biohorizons provide an age estimate for these two stratigraphic levels. The white dashed line on the density plot of *C. ehrenbergii* is a simplified interpreted trajectory of the highest population density intended to show the significant difference before and after 76 Ma.

#### 4.3. *M. undosus* relative abundance and size variations

*Microrhabdulus* spp. represent only a minor component of the calcareous nannofossil assemblage for much of the Coniacian to lower Campanian, where they are generally below 2.5% (Fig. 2). The relative abundance of the genus starts to increase up to 5% within the upper Campanian Zone CC21 and shows a first significant peak abundance in the top of CC21 and within Zone CC22 with values up to 9%. This significant increase in the relative abundance of the genus is actually related to the first common occurrence of *M. undosus* which is the dominant species within this lineage. *Microrhabdulus* spp. relative abundance fluctuates gently around 4% in the remaining of the upper Campanian. Above the

Campanian/Maastrichtian boundary, *Microrhabdulus* spp. increase and show a lower Maastrichtian acme with two double peaks of abundance reaching values as high as 12%. The top of this acme is in the upper part of zones CC25/UC19 and coincides with minimal values in *C. ehrenbergii*. Values then fluctuate between 1 and 7% in the remaining Maastrichtian (Fig. 2). The genus is essentially represented by two groups, *M. decoratus* and the *M. undosus* group. *M. decoratus* is responsible for a peak abundance of the genus up to 6% across the Coniacian/Santonian boundary. Otherwise, *M. decoratus* is generally below 1.5%, so the abundance fluctuations described above essentially correspond to that of the *M. undosus* group (Fig. 2). Variations in the length of the *M. undosus* group are generally biased by the frequent fragmentation observed for this species. *Microrhabdulus* nannoliths are elongated rods generally  $>10\ \mu\text{m}$  in length for 1 to 3  $\mu\text{m}$  in width, hence the rods are commonly fragmented and edges of the rod often lack the typical tapering observed in complete specimens. Despite this bias, the maximum length observed in each sample can still represent a valuable index as this parameter is more likely to represent the length of complete, non-fragmented specimens, but evidently, the average length is meaningless and hence, not considered further in this study. A major shift in the morphology of the *M. undosus* group occurs in the upper Campanian Zone CC22 in coincidence with the shift in the size of *C. ehrenbergii* and with a peak abundance of *Microrhabdulus* spp. (Fig. 3). This change is expressed by a significant increase in the width of the rod (Figs 3 and 4), together with the occurrence of specimens with wavy patterns in the extinction line of the central axis of the rod and a slight change in morphology of the laths from triangular to rose-thorn shaped (Fig. 4). Moreover, we also observe an increase in maximum length of our specimens that parallels the increase in width of the rod (Fig. 6).

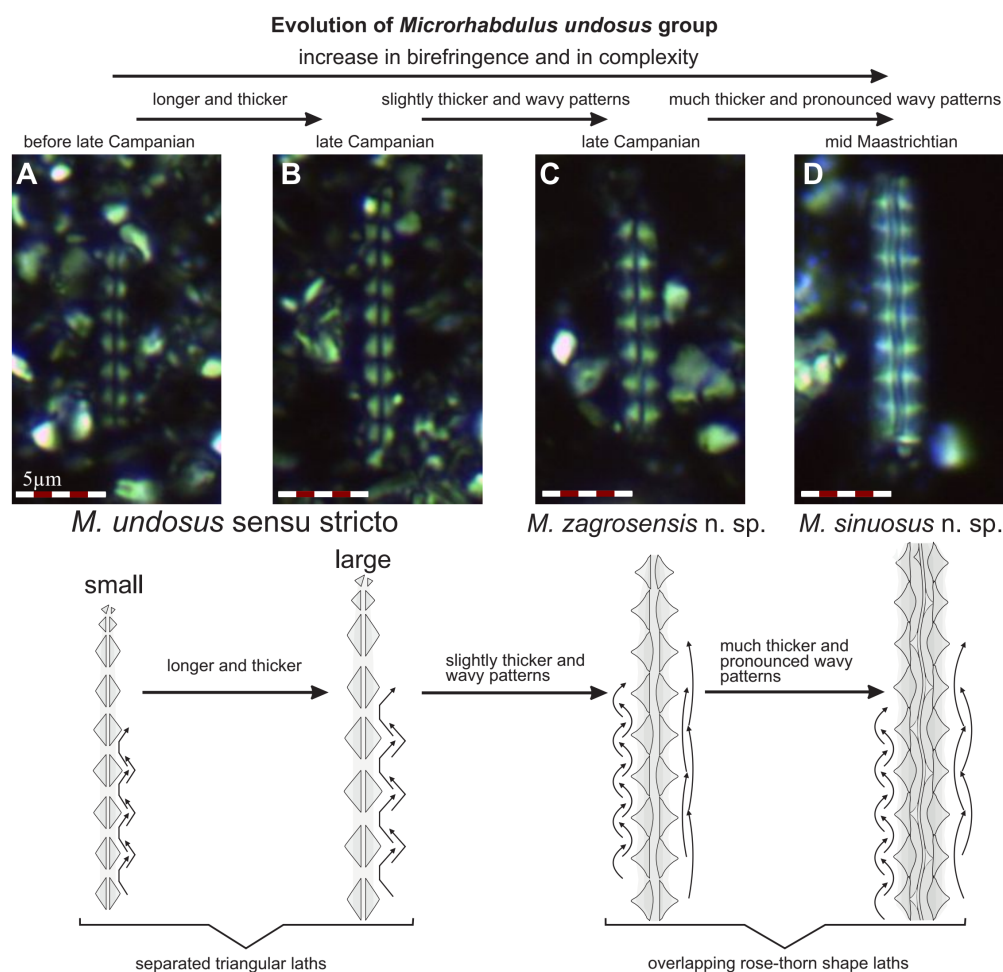


**Figure 4.** Evolution of the *Microrhabdulus undosus* group across the Campanian-Maastrichtian interval of the Shahneshin section with all distinctive features that characterize narrow (A) and large *M. undosus sensu stricto* (B), *Microrhabdulus zagrosensis* n. sp. (C) and *Microrhabdulus sinuosus* n. sp. (D).

It must be noted that the observed range of maximum length observed here varies between 14 and 27  $\mu\text{m}$  which matches the given rod size range of 15 to 30  $\mu\text{m}$  in illustrated specimens of the Nannotax3 database:

([https://www.mikrotax.org/Nannotax3/index.php?taxon=Microrhabdulus%20undosus&module=ntax\\_mesozoic](https://www.mikrotax.org/Nannotax3/index.php?taxon=Microrhabdulus%20undosus&module=ntax_mesozoic)).

A second episode with a significant change in morphology is observed at around 315 m, at the top of subzone CC25a/Zone UC19. The maximum length of the *M. undosus* group increases significantly to reach up to 27  $\mu\text{m}$  towards the top Maastrichtian. In parallel, a progressive, significant increase in the width of the rod is also observed in the same interval (Figs 3 and 4), together with the occurrence of numerous forms that bear a sinuous central axis and additional, overlapping rows of rose-thorn shape laths visible within the central axis (Fig. 4). These observations lead us to define two new species *Microrhabdulus zagrosensis* and *Microrhabdulus sinuosus* and append the definition of *M. undosus* sensu stricto (see section 4.1., taxonomy). The significant difference in distribution histograms of the *M. undosus* group below and above 240 m strongly supports the mixing of two or three distinct morphospecies in samples above 240 m (Fig. 5, distribution histograms C and D). We also produced distribution histograms for the width of the three distinguished morphospecies following the taxonomy given in the next chapter (Fig. 6, distribution histograms A, B, and C).

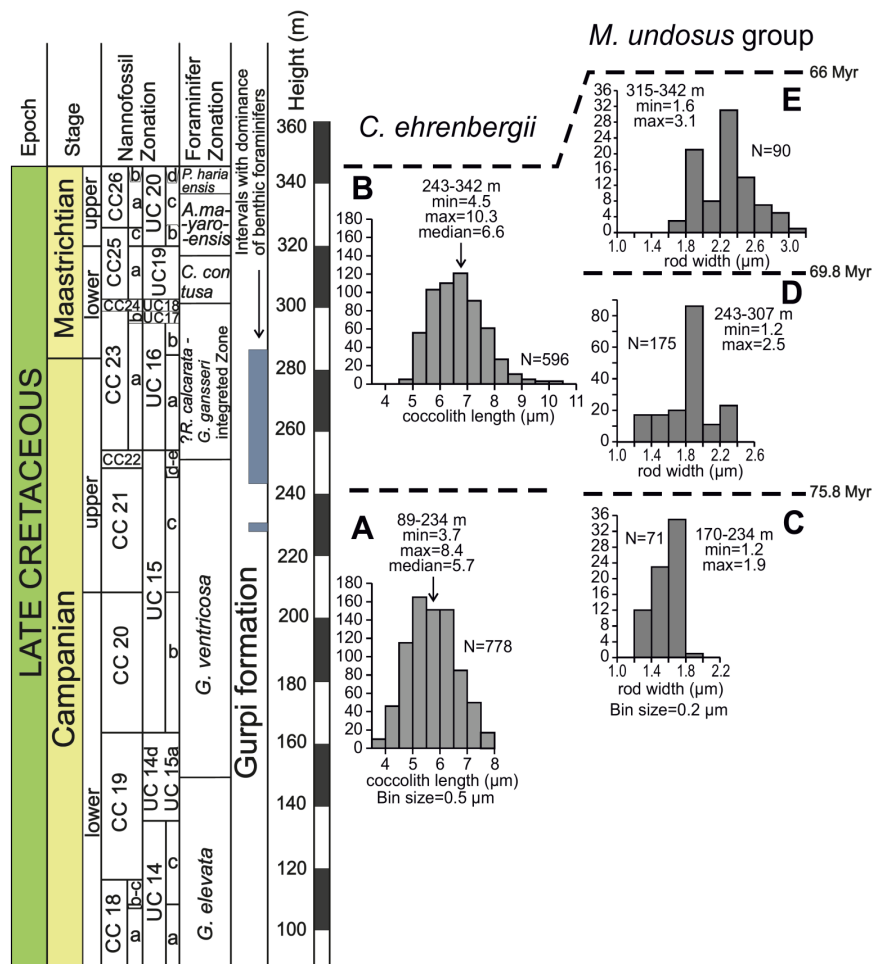


**Figure 5.** Distribution histograms of *C. ehrenbergii* (A and B) and *M. undosus* group (C, D and E) across relevant stratigraphic intervals highlighting observed differences in their morphology through time.



## 5. DISCUSSION

### 5.1. Taxonomy

Family AXOPODORHABDACEAE Wind and Wise in Wise & Wind (1977)

Genus *Cribrosphaerella* Deflandre in Piveteau (1952)

*Cribrosphaerella ehrenbergii*, (Arkhangelsky, 1912) Deflandre in Piveteau (1952)

Figure 7

**Remarks.** Reinhardt (1964) first made a distinction between distinct forms of Maastrichtian *Cribrosphaerella* species and this distinction was confirmed later on by Perch-Nielsen (1968) in the Maastrichtian of Denmark. In particular, they noticed a distinction between *C. ehrenbergii* and *C. hilli* based on the number of elements composing the shield, *C. hilli* having a clear tendency towards bearing more elements on the shield than *C. ehrenbergii*.

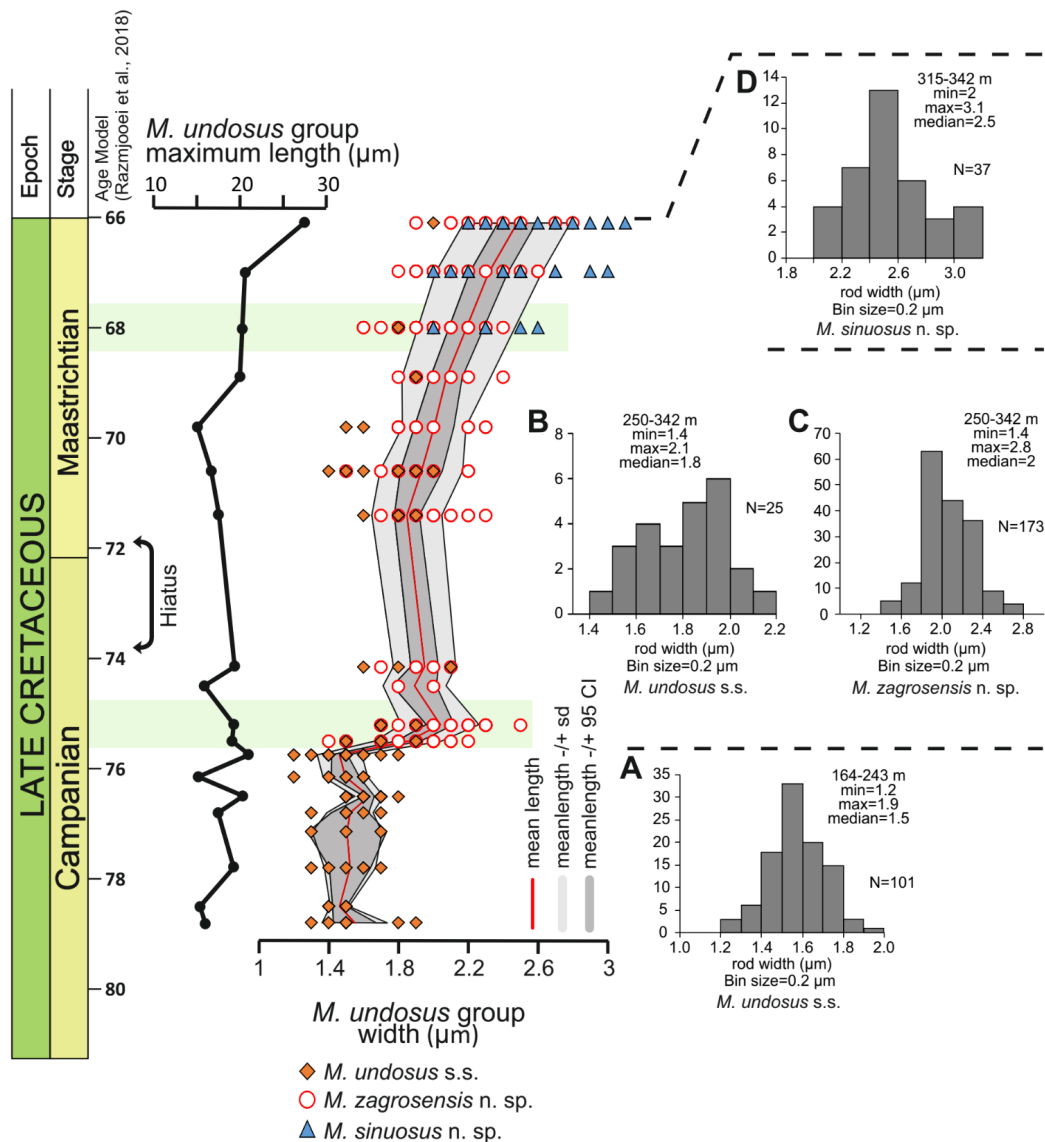


**Figure 6.** Maximum length, mean width, standard deviation and 95% confidence interval envelopes for measurements of the *Microrhabdulus undosus* group specimens along with the distribution histograms of three distinct morphospecies *M. undosus* (A and B), *Microrhabdulus zagrosensis* n. sp. (C) and *Microrhabdulus sinuosus* n. sp. (D) across the Campanian-Maastrichtian time interval. The colored data dots point to the three distinct morphospecies.

In her SEM illustrations, *C. hilli* appeared more elliptical than subrectangular, contrary to *C. ehrenbergii*, which was clearly subrectangular. Reinhardt (1964) and Perch-Nielsen (1968) did not mention any significant difference in size between *C. ehrenbergii* and *C. hilli*, but Perch-Nielsen (1968) showed that the minimum size of her measured specimens of *C. hilli* was 7  $\mu\text{m}$  long whereas her smaller specimen of *C. ehrenbergii* is 5  $\mu\text{m}$  long. The definition of *C. hilli* by Reinhardt (1964) provides a range of large sizes between 8 and 10  $\mu\text{m}$ , thus pointing towards systematically large specimens of *Cribrosphaerella* as compared to a total size range of 5-10  $\mu\text{m}$  for *C. ehrenbergii*. Therefore, we cannot completely exclude that our observation of a significant rise in the mean length of *C. ehrenbergii* recorded in the late Campanian of Shahneshin is possibly due to the first occurrence of *C. hilli*, this species is probably slightly bigger than *C. ehrenbergii*. We were not able to make any clear consistent distinction here in the outline (subrectangular versus elliptical) between our measured specimens of *C. ehrenbergii* in our investigations under XPL (Fig. 7).

Family MICRORHABDULACEAE Deflandre, 1963

Genus *Microrhabdulus* Deflandre, 1959

*Microrhabdulus undosus* Perch-Nielsen, 1973 emend. Razmjooei *et al.*

Figure 4A-B, Figure 8A-L, Figure 10C-D.

**Remarks.** All specimens measured in the present study were previously assigned to the species *M. undosus*. Morphological observations and measurements led us to redefine this group as a lineage that comprises three distinct species. From the detailed observations and biometric results obtained here, we redefined *M. undosus* sensu stricto (s.s.) as comprising narrow and large specimens of *Microrhabdulus* with undulating, slightly triangular laths and a neat, straight extinction line in the center of the rod when observed under XPL (Fig. 4). The sister species *M. decoratus* exhibits rows of strictly parallel-sided and butting, well-aligned laths of the same dimension under the SEM with no empty space in between distinct rows, and laths appearing as strictly rectangular under XPL with a straight extinction line in the center (Fig. 10A-B). Under the SEM, *M. undosus* s.s. exhibits less regular, non-strictly butting laths and visible open space in between the rows that allow observation of a preceding inner layer of laths beneath the outer layer (Fig. 10C-D). The resulting appearance of this morphology under XPL appears to be a characteristic slightly triangular aspect of the individual laths but we note that, in contrast to the two new species defined below, the central extinction line remains straight in *M. undosus* s.s. (Fig. 10C-D). In the Late Cretaceous of Shahneshin (Zagros, Iran), narrow and smaller specimens with a width of the rod measuring between 1.2 and 1.9  $\mu\text{m}$  (mean: 1.4  $\mu\text{m}$ ) and a maximum length of 20  $\mu\text{m}$  dominate in the lower Campanian and to the top of upper Campanian Zone CC21 (UC15c<sup>TP</sup>) (Figs. 3, 5 and 6). The uppermost Campanian specimens from Zone CC22 and Maastrichtian specimens are a bit wider, and vary in width between 1.4 and 2.1  $\mu\text{m}$  (mean 1.8  $\mu\text{m}$ ) but have a maximum length of 21  $\mu\text{m}$ , which is almost similar to narrower specimens (Figs 5, 6 and 8).

*Microrhabdulus zagrosensis* sp. nov.

Figures 4C, and 9A-9E, Figure 10E-F.

**Derivation of name.** Referring to the Zagros basin from which the species is hereby described.

**Diagnosis.** A long, wide species of *Microrhabdulus* with rose-thorn-shaped laths with pronounced wavy patterns of the laths and a central extinction line that starts to deviate from a straight line, when observed in XPL (Fig. 4 and Fig. 9A-E). Under SEM, we noticed open spaces in-between rows of laths as in *M. undosus* s.s., but more variations in the thickness of the individual laths with rows composed of thicker laths surrounding rows composed of thinner laths (Fig. 10F). Also, the width of the space between distinct rows can vary (Fig. 10E-F).

**Differentiation.** This species greatly resembles *M. undosus* s.s., from which it originates but can be distinguished from the latter by the rose-thorn shape of the laths under XPL, *M. undosus* sensu stricto bearing triangular laths; and by the wavy pattern of the extinction line of the central axis (Fig. 9A-E), *M. undosus* sensu stricto bearing essentially straight central extinction lines. *Microrhabdulus zagrosensis* differs from the newly defined *Microrhabdulus sinuosus* by the lack of any additional rows of laths in the central axis and by a narrower diameter of the rod. Under the SEM, the space left between two distinct upper/outer rows of laths is wider in *Microrhabdulus zagrosensis* compared to *M. undosus* s.s., but is narrower compared to *Microrhabdulus sinuosus* (Fig. 10).

In the Late Cretaceous of Shahneshin (Zagros, Iran), *Microrhabdulus zagrosensis* has a maximum length of 21  $\mu\text{m}$  and a width that varies between 1.4 and 2.8  $\mu\text{m}$  (mean of 2  $\mu\text{m}$ ) (Fig. 6).

*Holotype*. Figure 4C and 9A (L= 8.6  $\mu\text{m}$ , W= 1.8  $\mu\text{m}$ ).

*Paratypes*. Figure 9B, 9C, 9D and 9E.

*Type locality*. Shahneshin, central Zagros, Iran.

*Type level*. sample ShG2518, 258 m, Upper Campanian (Zone CC23a/UC16a<sup>TP</sup>).

*Occurrence*. Shahneshin; First occurrence is recorded in the upper Campanian CC22 Zone (UC15d-e<sup>TP</sup>) and last occurrence at the Cretaceous-Paleogene boundary.

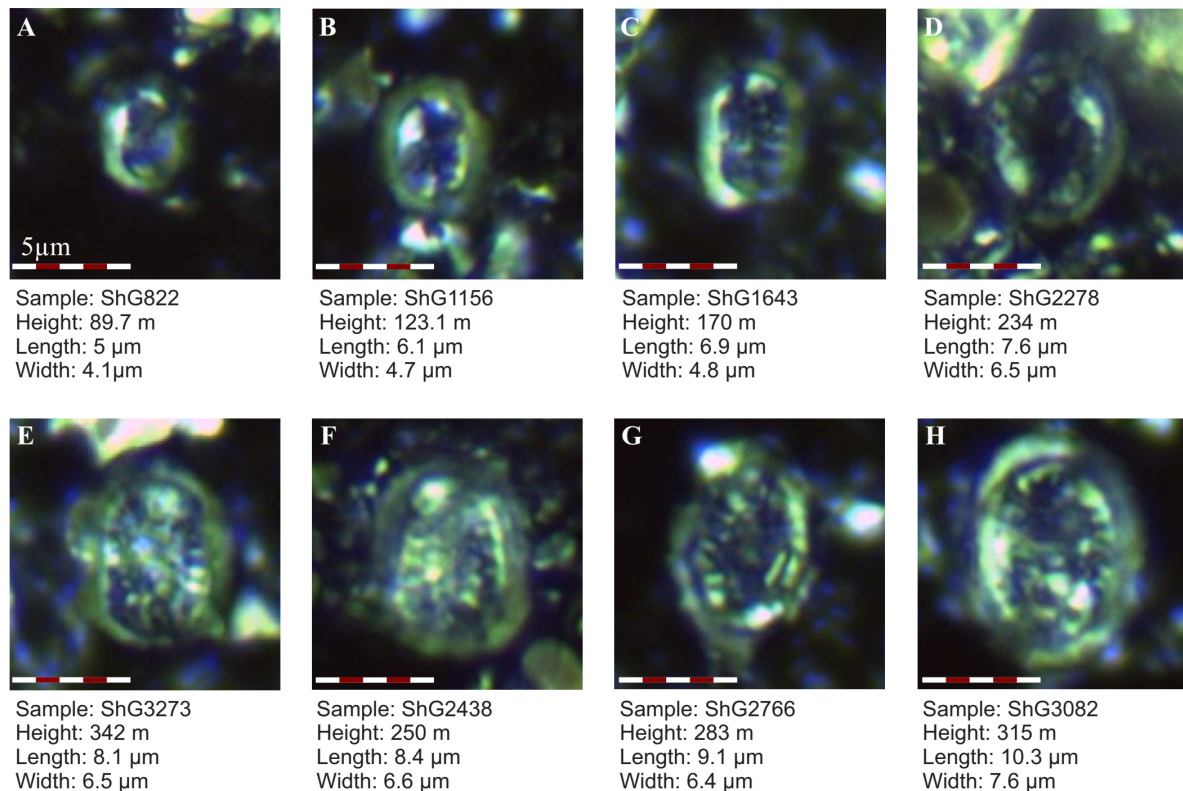


**Figure 7.** Selected *Cribrosphaerella ehrenbergii* specimens ordered from small to large forms.

*Microrhabdulus sinuosus* sp. nov.  
Figures 4D, and 9G - 9L, Figure 10G - I.

*Derivation of name*. Referring to the pronounced sinuosity of the central axis.

*Diagnosis*. A very long, thick species of *Microrhabdulus* with rose-thorn-shaped laths on the sides, much pronounced wavy patterns of the laths and bearing additional rows of laths that are visible in the central axis in XPL (Fig. 4 and Fig. 9G-L). As interpreted from our SEM observations, the strong wavy pattern of the laths under XPL is likely caused by the more complex undulating arrangement of the laths, with individual laths that vary slightly in width, hence they are less strictly rectangular in shape. There are also large open spaces between distinct rows of laths that allow observation of an inner layer and we notice some laths showing distinct kinks and/or trapezoidal shapes (Fig. 10H).

*Differentiation*. This species greatly resembles *M. undosus* s.s., but can be distinguished from the latter by the rose-thorn shape of the laths under XPL (*M. undosus* s.s. bearing triangular laths), by the much pronounced wavy pattern of the central axis (*M. undosus* s.s. bearing essentially straight extinction lines), and by the presence of additional rows of laths visible in the central axis (*M. undosus* s.s. showing a simple extinction line in this axis). *M. sinuosus* differs from the newly defined *M. zagrosensis* by a slightly wider diameter of the rod and the systematic presence of an additional row of laths in the central axis (Fig. 9G-L), feature that is absent in *M. zagrosensis* (Fig. 9A-E). Under the SEM, the spaces between two distinct

rows of laths in *M. sinuosus* appear wider than those in *M. undosus* and *M. zagrosensis*, and the laths composing the outer rows vary in width along the row, creating strong undulations that are likely responsible for the pronounced wavy patterns observed in XPL. The maximum length of *M. sinuosus* is greater than that of *M. zagrosensis* and *M. undosus* s.s., suggesting that the complete, non-fragmented specimens of the species essentially represent a giant species of *Microrhabdulus*. In the Late Cretaceous of Shahneshin (Zagros, Iran), *Microrhabdulus sinuosus* has a maximum length of 27  $\mu\text{m}$  and a width that varies between 2 and 3.2  $\mu\text{m}$  (mean of 2.5  $\mu\text{m}$ ) (Fig. 6).

**Remarks.** Note that there is likely a continuum in the evolution from *M. zagrosensis* to *M. sinuosus* as expressed by the progressive Maastrichtian increase in the diameter of the rod delineated in our data as well as by the presence of rare transitional forms that show very slightly undulating median extinction lines as in *M. zagrosensis* together with a faint additional row of laths in the center visible only in the upper third of the specimen (Fig. 9F).

**Holotype.** Figure 4D and 9G (L= 14.3  $\mu\text{m}$ , W= 2.7  $\mu\text{m}$ ).

**Paratypes.** Figure 9H, 9I, 9J, 9K and 9L.

**Type locality.** Shahneshin, central Zagros, Iran.

**Type level.** sample ShG3273, 342 m, late Maastrichtian (Zone CC26a/UC20c<sup>TP</sup>).

**Occurrence.** Shahneshin; First occurrence is recorded in the upper part of early Maastrichtian CC25a subzone (top of UC19) and last occurrence at the Cretaceous-Paleogene boundary.

## 5.2. Possible causes of morphological change in calcareous nannoplankton

### 5.2.1. Lessons from the Meso-Cenozoic

Important lessons for understanding coccolith size changes and their potential causes have been brought by the study of the three main Cenozoic genera of coccolithophores (*Reticulofenestra*, *Cyclargolithus*, and *Coccolithus*), namely that coccolith size is strongly linearly correlated to coccosphere and cell-diameter, and hence reflect changes in calcareous phytoplankton cell size (Henderiks, 2008). Out of these three genera, the Paleogene trend towards smaller reticulofenestrid cells across the Eocene to Miocene has been primarily interpreted as reflecting an adaptive response to increase aqueous CO<sub>2</sub> limitation caused by a decrease in atmospheric pCO<sub>2</sub> (Henderiks & Pagani, 2008; Hannisdal et al., 2012). As such, these cell size changes appear to be linked to coccolithophore calcification and cell growth. However, other factors have been postulated as potential controls on coccolith sizes and varying responses have been observed in distinct taxa. For instance, while the genus *Toweius* sees a decrease in coccolith length interpreted as a response to a rise in temperature and pCO<sub>2</sub> across the Paleocene/Eocene Thermal Maximum (PETM), *Coccolithus pelagicus* increases in size across that interval, which has been interpreted as a response to slowed cell division (O'Dea et al., 2014). Cyclic, rapid Pleistocene changes in the size of *Noelaerhabdaceae* have been related to species radiation and pulses of extinction (Bendif et al., 2019), but also to orbital changes in insolation for the past 400 kyr, with enhanced seasonality at insolation highs favoring speciation, expressed in biometric data by a larger range of coccolith sizes with distinct small and large populations (Beaufort et al., 2021). Lessons from the Cenozoic hence tend to show that prominent, rapid coccolithophore size changes primarily reflect episodes of speciation favored by climate change, but also possible long-term responses to changes in pCO<sub>2</sub> via calcification or cell growth rate.

In contrast, biometric studies in the Mesozoic tend to show a wider variety of possible controls on calcareous phytoplankton size variations. Cyclic changes in the size of Pliensbachian *Crepidolithus crassus* have been related to an orbital control, but the primary causes evoked to explain these features are changes in water turbidity and nutrient recycling in the photic zone via orbitally-controlled storm intensity (Suchéras-Marx et al., 2010). Large Pliensbachian nannolith *Schizosphaerella* size changes have been interpreted as variations in abundance of three distinct morphotypes as a response to variations in temperature and proximity to the coastline (Peti & Thibault, 2017; Peti et al., 2021), whereas the drop in size of this same taxon across the Toarcian Oceanic Anoxic Event has been interpreted as a response to a calcification crisis (Suan et al., 2010; Clémence et al., 2015; Faucher et al., 2022). Changes in the size of Early to Middle Jurassic coccolith *Lotharingius* species might reflect the opposition between stable environmental conditions favoring large specimens versus periods dominated by ecological stress favoring small specimens (Ferreira et al., 2017). Mid-Cretaceous size changes in *Biscutum constans* have been interpreted as a response to both temperature variations and environmental stability versus altered ocean



chemistry from widespread volcanism (Bottini & Faucher, 2020). In contrast, size changes in *B. constans*, *Rhagodiscus asper* and *W. barnesiae* across a mid-Barremian episode of black shale deposition in the Boreal Realm have been primarily interpreted as a response to changes in nutrients (Wulff et al., 2020). Despite the large variety of causes invoked in Mesozoic studies to explain the latter morphological changes, putative distinct morphotypes and hence pseudo-cryptic paleontological species have often been inferred and such variations in size appear correlated to pronounced climatic and environmental changes.

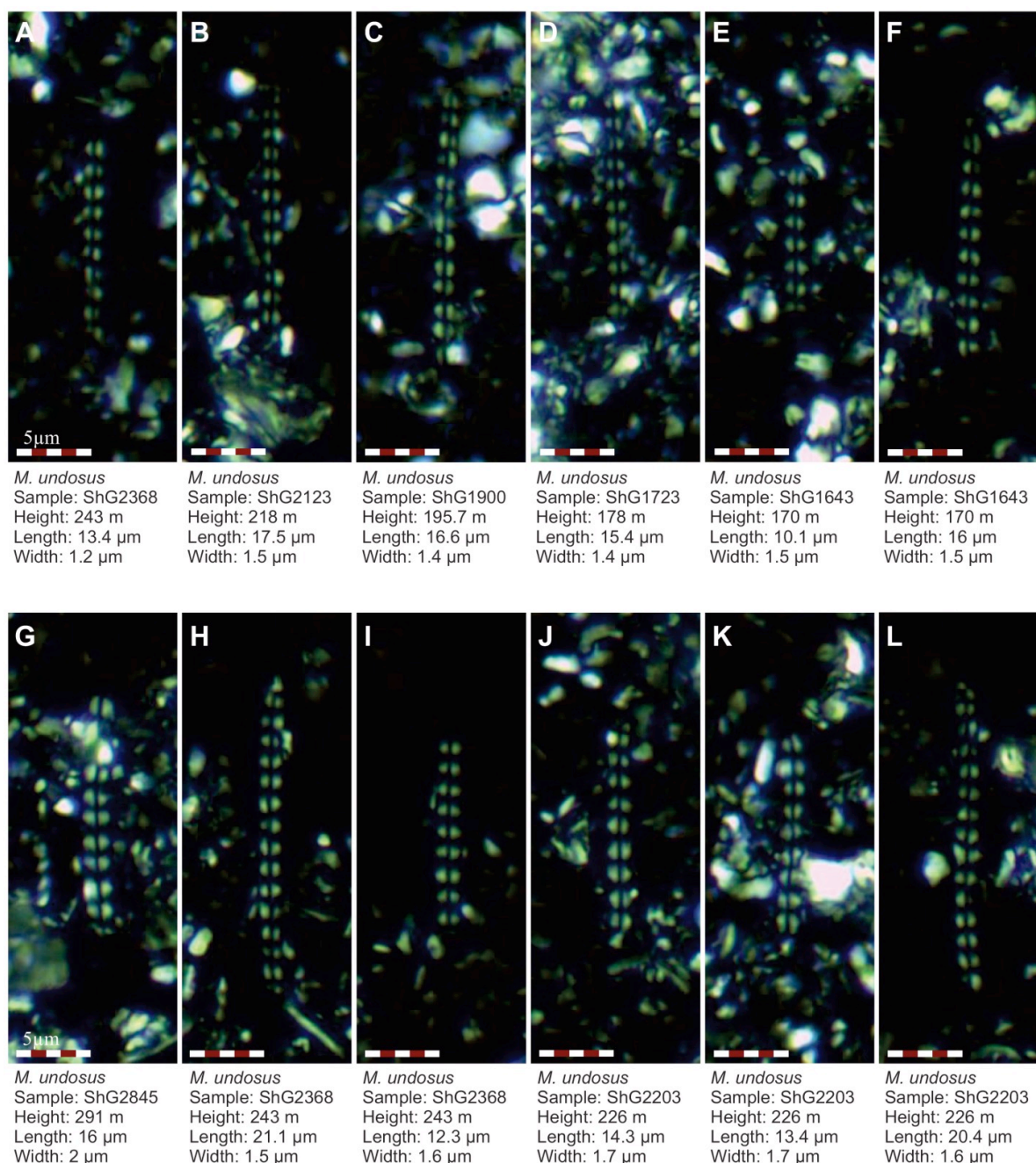


**Figure 8.** Selected small and narrow forms (A to F; before CC22 zone) and large and wide forms (G to L; after CC21 zone) of *Microrhabdulus undosus* in the Shahneshin section.



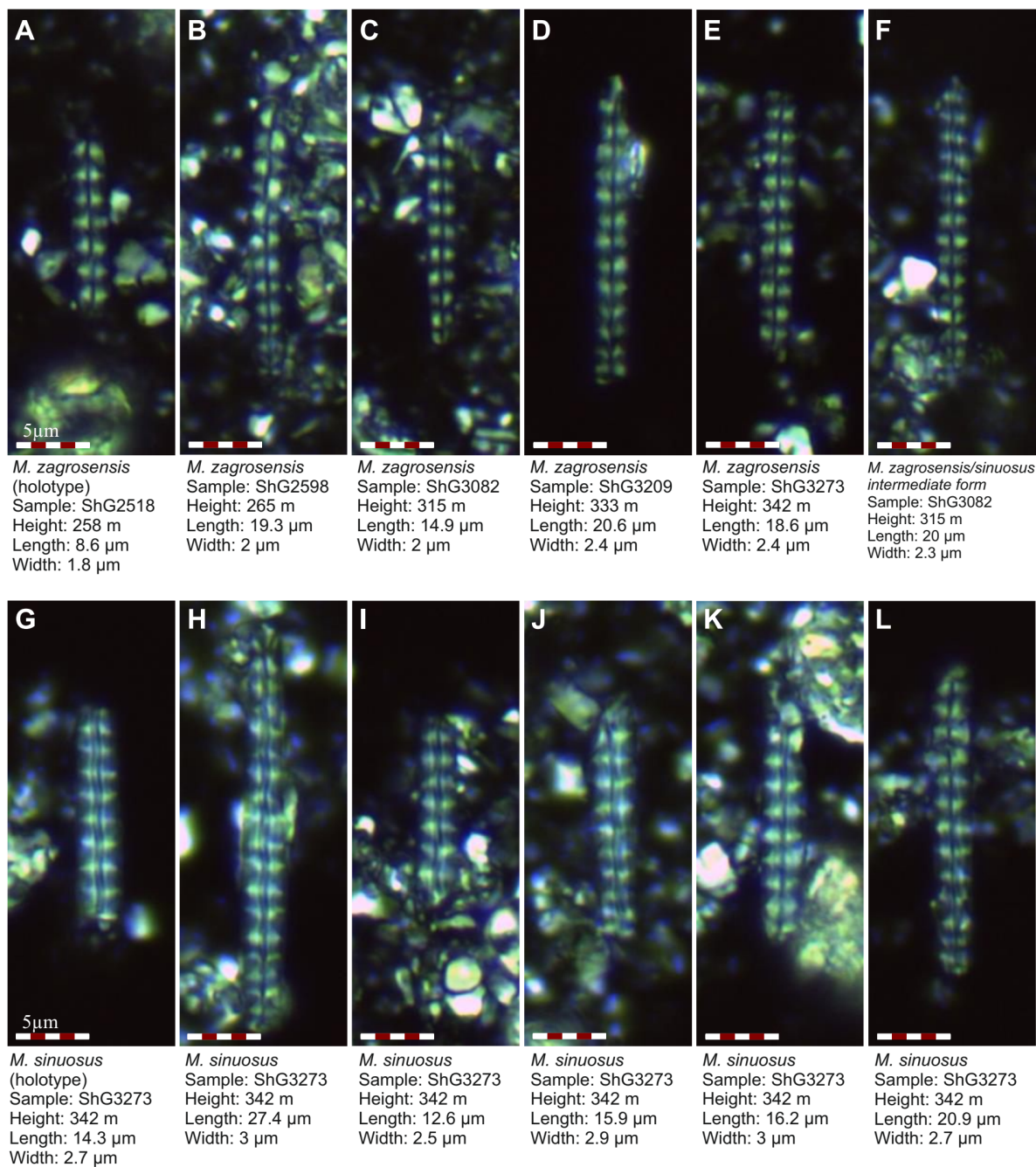


**Figure 9.** The selected holotype (A) and paratypes (B to E) of *Microrhabdulus zagrosensis* sp. nov. and holotype (G) and paratypes (H to K) of *Microrhabdulus sinuosus* sp. nov., in the Shahneshin section. Picture F also presents an intermediate form between the two newly defined species.

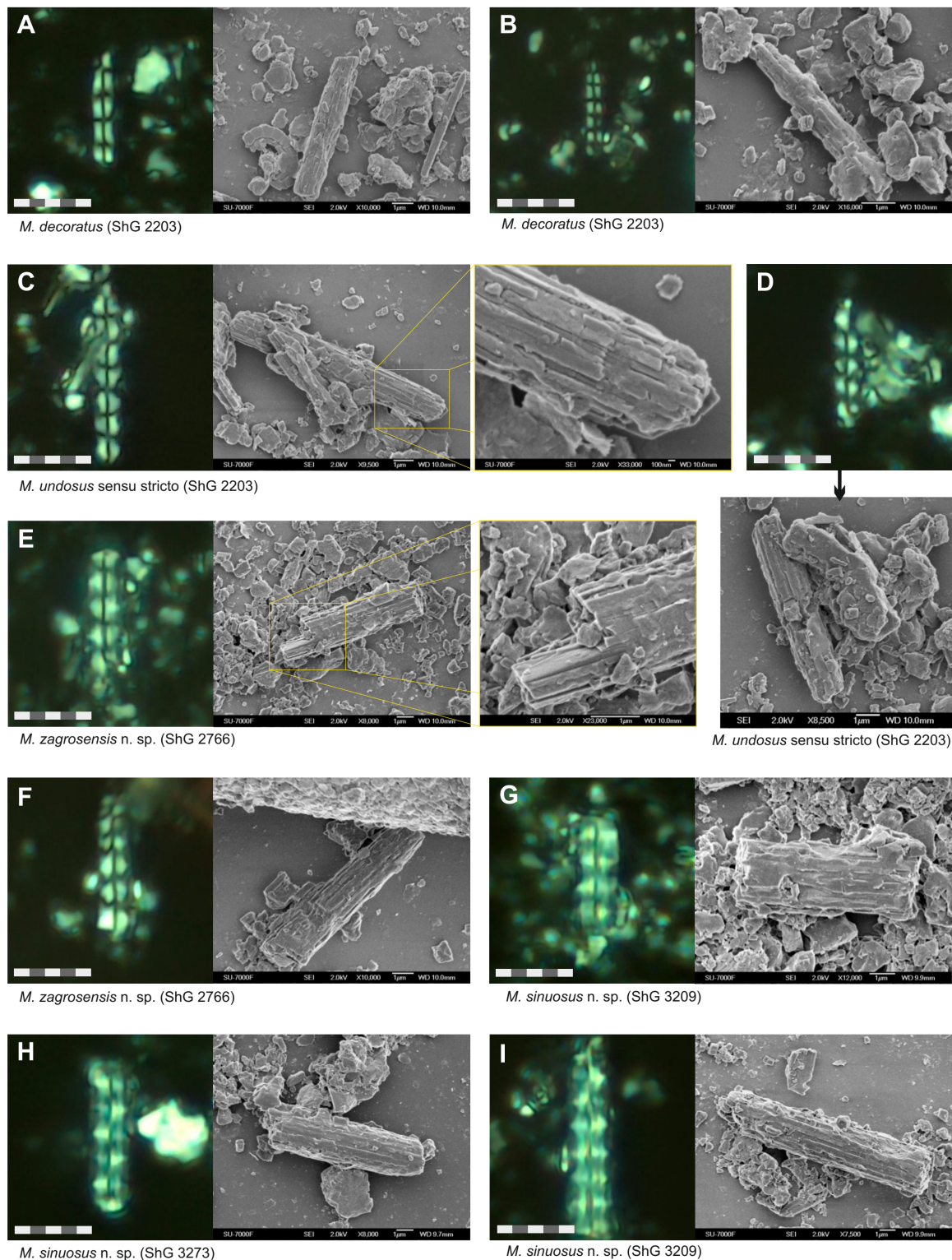


**Figure 10.** The selected pictures of the same individuals of *Microrhabdulus* specimens observed under the light microscope (XPL) and SEM.

### 5.2.2. Are Cope-Bergmann's rules applicable to phytoplankton?

Aubry et al. (2005) demonstrated that the average size of coccoliths has increased from the Early Jurassic through the Santonian, stabilized until the Campanian and then decreased during the Maastrichtian. Remarkably, they noticed that this size history parallels the diversity (species richness) history of the Mesozoic Coccolithophorids. Consequently, these authors claimed that these observations



constitute an illustration of Cope's rule. The same idea was later reiterated for a number of Jurassic-Cretaceous coccolith taxa (López-Otálvaro et al., 2012; Ferreira et al., 2017; Gollain et al., 2019).

Cope's rule postulates that "evolution proceeds in the direction of increasing body size" (Ghiselin, 1972, p. 141). In parallel, another rule of evolution in organisms named Bergmann's rule stipulates that organisms evolve larger sizes under cold temperatures (Timofeev, 2001; Meiri & Dayan, 2003). This correlation between body size and temperature variations led to the idea of an integrated Cope-Bergmann hypothesis, suggesting that Cope's rule may simply be an evolutionary manifestation of Bergmann's rule (Hunt & Roy, 2006). Cope-Bergmann hypothesis predicts that the size of organisms increases in relation to climatic cooling, and it was applied to micro-organisms such as verified in Cenozoic deep sea ostracods (Hunt & Roy, 2006) and even Cenozoic planktonic foraminifera (Schmidt et al., 2004, 2006).

However, Cope's rule implies a number of causal factors to the increase of body size through time (such as endothermy and prey-predator relationships) that only applies to multicellular organisms with sexual reproduction (Hone & Benton, 2005). Moreover, a common character of Cope's rule is the observation that the general increase in body size operates at the level of higher clades such as classes and orders but not particularly at the level of lower clades down to the family, genera, and species (Novack-Gottshall & Lanier, 2008). This is therefore in strong contrast to unicellular calcareous phytoplankton for which we see a transient increase in cell size within lower clade levels as exemplified in many examples of the literature given above. Similarly, Bergmann's rule has been essentially evoked in animal evolution, and causal factors of this rule involve temperature regulation as the primary adaptive mechanism for this rule is a decrease in the surface area to volume ratio, reducing heat loss in colder conditions (Timofeev, 2001; Meiri & Dayan, 2003). These implications make it difficult to apply this rule blindly to unicellular phytoplanktonic organisms that are essentially eurythermal.

Finally, although observations by Aubry et al. (2005) on the size of Mesozoic coccolithophorids are undeniable, a counter-example by the same prime author was given for the Neogene where most lineages of coccolithophorids underwent a general decrease in size in parallel to a long-term cooling trend, in strong contrast with the Cope-Bergmann hypothesis (Aubry, 2009). The applicability of Cope-Bergmann's hypothesis to calcareous nannoplankton thus appears questionable, both due to the counter-examples occurring in various lineages of this group, and to the causal factors that this rule implies which operate at a higher level than the cell and higher taxonomic ranks.

However, some analogy might be drawn in our understanding of how climate change affects biodiversity because, as recently demonstrated in the Quaternary, rapid phenotypic size changes in calcareous nannoplankton almost always imply speciation events, which appear to be related to significant climate changes (Bendif et al., 2019; Beaufort et al., 2022). Moreover, direct causal factors that can be invoked for size variation in plankton may be indirectly related to temperature and, in fact, driven by other factors, like fertility and light availability. Since the density of cold water is higher than warm water, a probable explanation for the size variation in plankton through geological time could be changing in buoyancy (Eppley et al., 1967; Walsby & Reynolds, 1980). In cold periods, calcareous nannoplankton may be able to compensate for some of the effects of increasing buoyancy by increasing their size and consequently their weight. This is especially the case for those phytoplanktons that only can tolerate a specific range of light intensity, so the increasing size would allow them to sink to levels where light intensity is suitable (see Morgan & Kalf, 1979; Meeson & Sweeney, 1982; Atkinson 1994). On this basis, phytoplankton species that cannot adjust their size with buoyancy variation may become extinct, while those with wider light intensity tolerance may show no change in size.

### 5.3. Are morphological changes in *C. ehrenbergii* and *M. undosus* lineages related to climatically-controlled episodes of speciation?

If rapid phenotypic size changes observed in calcareous nannoplankton lineages often result from diversification, then short- and long-term climate and environmental changes likely operate as causal factors via biogeographical partitioning. A compilation of calcareous nannoplankton diversity through time (Bown et al., 2004) allowed Bown (2005) to suggest that Cretaceous nannoplankton diversification occurred during cold intervals, supported by increased paleobiogeographical partitioning of oceanic photic-zone environments and the establishment of high-latitude provinces.

### 5.3.1. A possible relationship with the peak in global nannoplankton diversity at 76 Ma

We cannot exclude that the observed shift in the size of *C. ehrenbergii* reflects the origination of a new, larger species that became common in the late Campanian-Maastrichtian (possibly *C. hilli*, see taxonomy in section 4.1). We notice that this size change is relatively fast in the term of geologic time (less than 500 kyr, Supplementary Appendices 3 and 4, and Fig. 3), and the length of *C. ehrenbergii* remains almost constant around the same average after the shift (Fig. 3). Such a pattern is quite typical of Gould & Eldredge (1977) punctuated equilibrium model characterized by long periods of stasis punctuated by rapid shifts in morphology interpreted as evolutionary pulses. Such patterns are common in coccolithophores (Knappertsbusch, 2000; Geisen et al., 2004). Remarkably, the timing of the shift in size from a mean of around 5.5 to 6.5  $\mu\text{m}$  in *C. ehrenbergii* coincides with the first occurrence (FO) of *Microrhabdulus zagrosensis* which also corresponds to a transient, rapid shift in morphology of the *M. undosus* group. *Microrhabdulus* rods resemble in many ways central processes observed in many coccolith lineages and bear various morphologies. However, it has never been found attached so far to a Cretaceous coccolith and the origin of this nannolith lineage remains obscure. Hence, size changes related to *M. undosus* cannot be attributed with confidence to any putative changes in the cell size of a fossil phytoplanktonic algal group. Rapid changes observed in this taxon can at best represent episodes of diversification within the lineage. The coincidence in the timing of the rapid increase in *C. ehrenbergii* and the emergence of *M. zagrosensis* can be dated at around 76 Ma thanks to the first occurrences of *R. cf. R. calcarata* (planktonic foraminifera) and *Uniplanarius trifidus* at around 250 m (Fig. 3). Moreover, the timing of these events also coincides with a significant increase in the abundance of benthic foraminifera in the Shahneshin section that was interpreted as a relative sea-level low (Razmjooei et al., 2018) and correlates precisely with a global sea-level low delineated in the Miller et al. (2005) sea-level estimates of New Jersey (details in Kominz et al., 2008, figure 10). We cannot exclude that the apparent rapidity of what we interpret as an evolutionary pulse in both *C. ehrenbergii* and *M. undosus* group is due to a hiatus in nannofossil Zone CC22 associated with this sea-level low. Nevertheless, the coincidence of these morphological shifts in both lineages suggests a possible common external forcing on nannoplankton evolution.

Figure 11 summarizes the results obtained in our study, updates the phylogeny of *Microrhabdulus* through the Late Cretaceous and compares these evolutionary trends to (1) the recent TEX<sub>86</sub> compilation of O'Brien et al. (2017), (2) the compilation of bulk carbonate carbon isotopes drawn from the Late Cretaceous English chalk standard of Jarvis (2006) and the late Campanian-Maastrichtian Danish chalk (Thibault et al., 2012; 2016) and (3) Bown et al. (2004) global diversity of calcareous nannofossils. This figure supports a strong link between rises in the global diversity of nannoplankton and cooling intervals in the lower Cenomanian as well as in the Santonian to Maastrichtian. In particular, the peak of global diversity reached at 76 Ma corresponds broadly to an episode of acceleration of surface-water cooling in the late Campanian and to the so-called Late Campanian Event, a ca. 1 per mil negative carbon isotope excursion (Fig. 11). This timing corresponds exactly to that of the positive shift in the sizes of *C. ehrenbergii* and *M. undosus* and to the first occurrence of *Microrhabdulus zagrosensis* (Figs 5 and 6). We infer here that our observations illustrate an intimate link between climatic cooling, the Campanian carbon cycle and speciation, and strongly support that the Late Cretaceous nannoplankton peak in diversity was essentially fueled by cooling. The rise in diversity that appears to precede this interval centered around 76 Ma is most likely due to the wide binned average used to draw nannofossil global diversity. Both *C. ehrenbergii* and *M. undosus* groups show a significant increase in relative abundance through the late Campanian to Maastrichtian interval and the onset of this increase coincides with the shift in morphology observed in both taxa at 76 Ma.

The late Campanian acceleration of cooling and associated Late Campanian carbon isotope event around 76 Ma have been linked to tectonic uplifts and formation of reliefs around the Tethys, enhancing atmospheric CO<sub>2</sub> consumption by increasing continental weathering and erosion (Chenot et al., 2016, 2018; Corentin et al., 2022). Such a supra-regional tectonic uplift associated with a global sea-level low not only could have a prominent role in reducing global temperature but could also have a significant effect on sea-surface water fertility and oceanic circulation in Tethys. In such conditions, a bigger cell size could have been advantageous in environments with high nutrient availability since as cell size increases, the surface-to-volume ratio decreases, and the ability to obtain nutrients and light decreases (e.g., Marañón, 2015). Hence, considering the fact that nutrient supply and light availability are regarded as two crucial factors in controlling modern phytoplankton size structure (e.g., Marañón, 2015), the record of size changes in our

study may not be explained by temperature alone. The transient increase in abundance of *C. ehrenbergii*, together with the emergence of larger *C. ehrenbergii* and *Microrhabdulus zagrosensis* across the late Campanian to early Maastrichtian matches well the cool Late Campanian Event (Fig. 11), and this episode might have triggered further modifications in the ocean circulation and structure, affecting the buoyancy of plankton, and fertility levels. This interaction could have increased the persistent selection pressure on calcareous nannoplankton toward phenotypic divergence and provincialism. The results of this work suggest that the peak in global nannoplankton diversity reached at 76 Ma could even be underestimated as very few of the numerous calcareous nannofossil lineages of the Campanian interval have been so far the object of consistent biometric studies.

### 5.3.2. Is the emergence of *M. sinuosus* related to the mid-Maastrichtian event?

One of the striking features of the Maastrichtian nannofossil zonal and subzonal schemes is a sudden shift from the neat dominance of biohorizons represented by last occurrences in the early Maastrichtian to the sole presence of first occurrence biohorizons in the late Maastrichtian interval. Thibault (2016) discussed this feature and showed that at least for the South Atlantic, the mid-Maastrichtian, and to a lesser extent the late Maastrichtian, are characterized by several discrete origination events. Several nannofossil species, including *Micula premolisilvae*, *Micula praemurus*, *Micula murus*, *Lithraphidites quadratus*, *Ceratolithoides amplexor* and *Ceratolithoides kamptneri* have been shown to first originate worldwide in the mid-Maastrichtian. This interval is also characterized by a significant increase in the size of the common genus *Arkhangelskiella* due to the massive occurrence of a large representative of this group (*A. maastrichtiensis* Burnett, 1997, syn. *A. cymbiformis* var. W, Varol, 1989; Thibault, 2010). The 2 myr-long bins of the estimated nannoplankton global diversity curve somewhat prevent the distinction of this event in the global compilation, but a clear increase in origination rate and diversity of nannofossils has been reported at the same time interval in the southern high latitudes and in the South Atlantic (Huber & Watkins, 1992; Thibault, 2016). This trend is also observed in planktonic foraminifera in the areas mentioned above as well as at low and middle latitudes (Boersma & Schackleton, 1981; Boersma, 1984; Caron, 1985; Huber, 1990, 1992; Li & Keller, 1998). Interestingly, the rise in the diversity of planktonic organisms appears to be paralleled by potential diversity increases in cephalopods (southwestern France-northern Spain, (Ward et al., 1991); northwest Pacific, (Jagt-Yazykova, 2011, 2012); Mexico, (Ifrim et al., 2004, 2010); Seymour Island, Antarctica, (Witts et al., 2015)) and bivalves (Seymour Island, Antarctica, (Macellari, 1988)), though non-regulated inoceramids and rudists suffered a significant decline during the same interval (Ward, 1990; MacLeod & Ward, 1990; MacLeod, 1994; Johnson & Kauffman, 1996). Such changes in diversity among independent lineages and clades reduce the plausibility of a taphonomical bias. Overall, this event is spread across the early/late Maastrichtian boundary interval over ca. 2 myr and spans the two transitions from the early Maastrichtian cooling event to the mid-Maastrichtian warming, and the mid-Maastrichtian warming to the late Maastrichtian cooling (Thibault, 2016). The first occurrence of *Microrhabdulus sinuosus* at around 69.25 Ma is inscribed into this general mid-Maastrichtian diversification event.

The Campanian/Maastrichtian transition and lower Maastrichtian are marked by a pronounced long-term global cooling (close to 7°C) paralleled by the decrease in global nannoplankton species richness following the late Campanian peak in diversity. While the Late Campanian cooling might have favored higher diversity via biogeographic partitioning, the following long-term trend of early Maastrichtian cooling could also be responsible for the extinction of a number of species that were better adapted to higher CO<sub>2</sub> levels and/or higher temperatures and fertility levels, such as the biostratigraphic markers *Reinhardtites levis*, *Tranolithus orionatus* and *Broinsonia parca constricta* (Thibault, 2016; Razmjooei et al., 2020b). In contrast, the widespread episode of speciation in mid-Maastrichtian planktonic organisms does not coincide with climatic cooling but rather with higher temperature instability when global climate rapidly shifted from cool to warmer temperatures to cool again, from 69 to 67 Ma (Li & Keller, 1998; Thibault et al., 2016). Thus, the processes at play here differ from the case of the late Campanian and may be better explained by the conjunction of globally cooler temperatures with temperature instability (Fig. 11). The cooler temperatures of the Late Cretaceous could have fostered a rapid evolution in many lineages by quickly changing the direction of selection. In contrast, the temperature instability of the mid-Maastrichtian may have enhanced climatic heterogeneity, and hence geographical heterogeneities and provincialism triggered phenotypic divergence in nannoplankton and many other marine groups.



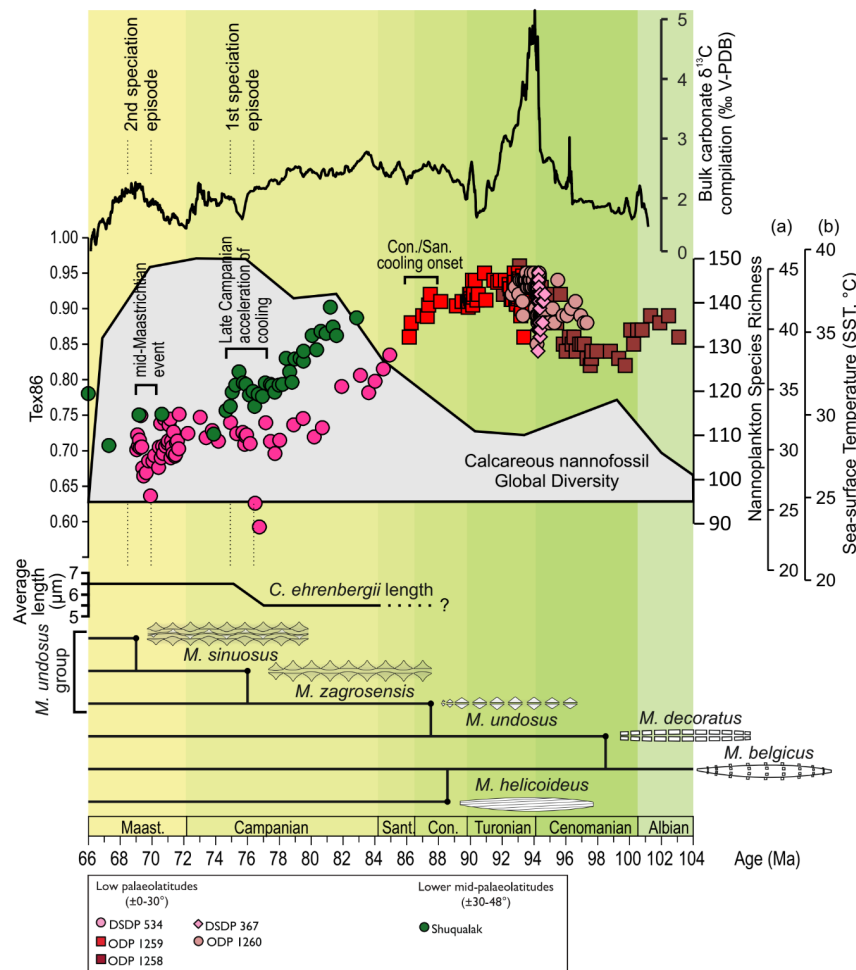


**Figure 11.** Schematic synthesis of data obtained in this study with a reconstructed phylogeny of the *Microrhabdulus* lineage, across the late Albian to Maastrichtian, and comparison with global changes in sea-surface temperatures from  $\text{TEX}_{86}$  (O'Brien et al., 2017), global calcareous nannoplankton diversity (Bown et al., 2004), and a standard bulk carbonate carbon isotope curve compiled from the English chalk standard of Jarvis (2006) and the late Campanian-Maastrichtian curve of the Danish Basin from Thibault et al. (2012, 2016). The phylogeny of *Microrhabdulus* is based on Nannotax website (Young et al., 2017). Two distinct SST estimates derived from  $\text{TEX}_{86}$  are provided: (a)  $\text{TEX}_{86}^{\text{H}}$ -SST calibration and (b) linear  $\text{TEX}_{86}$ -SST calibration. See O'Brien et al. (2017) for details on these calibrations as well as for symbols used in the figure to distinguish the different deep-sea sites and sections used in this compilation.

## 6. Conclusions

Changes in the morphology of two Late Cretaceous nannofossil lineages have been investigated here in deposits from the Zagros Basin (Iran). A common event occurs at c. 76 Ma in the late Campanian with a sudden significant increase in the mean length of *C. ehrenbergii* and in the mean width, as well as a change in the shape of *M. undosus* that led us to define the emergence of *Microrhabdulus zagrosensis* n.sp. at that time. Later on, at c. 69 Ma in the mid-Maastrichtian, the second increase in mean width and maximum size of the *M. undosus* group lineage is observed, along with an increased complexity in the arrangement of the laths of the rod, leading us to define the emergence of *Microrhabdulus sinuosus* n.sp. Comparison of the timing of these morphological changes and emergence of new species with nannoplankton global diversity, global climate change and global patterns in planktonic organisms allowed us to suggest that these two origination events might illustrate so far hidden but significant episodes of morphological change linked to episodes of diversification within Late Cretaceous nannoplankton. Indeed, the first speciation event coincides with a global peak in nannoplankton diversity and a Campanian episode of acceleration of cooling

associated with the Late Campanian carbon isotope event, while the second episode coincides with the mid-Maastrichtian Event, a ~2 myr-long interval of climatic instability and ocean reorganization characterized by diversification in planktic organisms and several marine invertebrate groups, as well as by the extinction of non-regulate inoceramids. Our results call for a closer examination of potential morphological change within the numerous Santonian to Maastrichtian calcareous nannofossil lineages.

### Acknowledgements

We would like to thank Andrej Spiridonov and the anonymous reviewer for helpful reviews and comments that greatly improved the manuscript, and the recommender Emilia Jarochovska for handling the peer review process (<https://paleo.peercommunityin.org/articles/rec?id=47>). The authors are grateful to Marie-Pierre Aubry for her helpful suggestions and reviewing the manuscript.

### Funding

This study was funded by the Carlsberg foundation grant CF16-0457 “Expression of orbital climate change across major environmental perturbations: case studies from the Late Cretaceous”. Funding for the SEM work is provided by the Swedish Research Council (DNR- 2020-04379) grant awarded to Matt O'Regan.

### Competing interests

The authors declare they have no personal or financial conflict of interest relating to the content of this article.

### Data availability

Supporting data including biometric measurements and calculations are available in supplementary appendices 1, 2, 3 and 4. Any additional data may be provided by Mohammad Javad Razmjooei ([mj.razmjooei@gmail.com](mailto:mj.razmjooei@gmail.com)).

### Author contributions

MJR: studying the samples (100%), biometric measurements (100%), interpretations (30%), figures preparation (60%), writing the manuscript (30%).

NT: interpretations (70%), figures preparation (40%), writing the manuscript (70%). NT is the corresponding author because he has more dominance on the subject of manuscript.

### Supplementary Appendices

SUPPLEMENTARY APPENDIX 1: Biometric results of *Cribrosphaerella ehrenbergii* specimens in Campanian-Maastrichtian interval. <https://osf.io/htvc5/>

SUPPLEMENTARY APPENDIX 2: Biometric results of *Microrhabdulus undosus* group specimens in the late Campanian-Maastrichtian interval. <https://osf.io/htvc5/>

SUPPLEMENTARY APPENDIX 3: Age-depth model of the Shahneshtin section suggested by Razmjooei et al. (2018), and the position of studied samples for *C. ehrenbergii* species. GTS2016: Ogg et al. (2016). <https://osf.io/htvc5/>

SUPPLEMENTARY APPENDIX 4: Age-depth model of the Shahneshtin section suggested by Razmjooei et al. (2018), and the position of studied samples for *M. undosus* group. GTS2016: Ogg et al. (2016). <https://osf.io/htvc5/>

## References

- Arkhangelsky, A. D. (1912). Upper Cretaceous deposits of east European Russia. *Materialien zur Geologie Russlands*, 25, 1-631.
- Atkinson, D. (1994). Temperature and organism size: a biological law for ectotherms?. *Advances in ecological research*, 25, 1-58.
- Aubry, M. P., Bord, D., Beaufort, L., Kahn, A., and Boyd, S. (2005). Trends in size changes in the coccolithophorids, calcareous nannoplankton, during the Mesozoic: A pilot study. *Micropaleontology*, 51(4), 309-318. <https://doi.org/10.2113/gsmicropal.51.4.309>
- Aubry, M.P., (2009). A sea of Lilliputians, *Palaeogeography, Palaeoclimatology, Palaeoecology*, 284, 88–113. <https://doi.org/10.1016/j.palaeo.2009.08.020>
- Barbarin, N., Bonin, A., Mattioli, E., Pucéat, E., Cappetta, H., Gréselle, B., Pittet, B., Vennin, E. and Joachimski, M. (2012). Evidence for a complex Valanginian nannoconid decline in the Vocontian basin (South East France). *Marine Micropaleontology*, 84, 37-53. <https://doi.org/10.1016/j.marmicro.2011.11.005>
- Barrier, E., Vrielynck, B., Brouillet, J. F. and Brunet, M.F., (2018). Paleotectonic Reconstruction of the Central Tethyan Realm. *Commission for the Geological Map of the World: Paris, France*, 21.
- Beaufort, L., Bolton, C.T., Sarr, A.C., Suchéras-Marx, B., Rosenthal, Y., Donnadieu, Y., Barbarin, N., Bova, S., Cornuault, P., Gally, Y. and Gray, E., (2022). Cyclic evolution of phytoplankton forced by changes in tropical seasonality. *Nature*, 601(7891), 79-84. <https://doi.org/10.1038/s41586-021-04195-7>
- Bendif, E.M., Nevado, B., Wong, E.L., Hagino, K., Probert, I., Young, J.R., Rickaby, R.E. and Filatov, D.A., (2019). Repeated species radiations in the recent evolution of the key marine phytoplankton lineage *Gephyrocapsa*. *Nature communications*, 10(1), 1-9. <https://doi.org/10.1038/s41467-019-12169-7>
- Boersma, A. (1984). Cretaceous-Tertiary planktic foraminifers from the southeastern Atlantic, Walvis Ridge area, Deep Sea Drilling Project Leg 74. *Initial Report: DSDP*, 74, 501-523.
- Boersma, A., and Shackleton, N. J. (1981). Oxygen- and carbon-isotope variation and planktonic-foraminifera depth habitats, late Cretaceous to Paleocene, Central Pacific, Deep Sea Drilling Project Sites 463 and 465. *Initial Report: DSDP*, 62, 513-526.
- Bollmann, J. (1997). Morphology and biogeography of *Gephyrocapsa* coccoliths in Holocene sediments. *Marine Micropaleontology*, 29, 319-350. [https://doi.org/10.1016/S0377-8398\(96\)00028-X](https://doi.org/10.1016/S0377-8398(96)00028-X)
- Bornemann, A. and Mutterlose, J., (2006). Size analyses of the coccolith species *Biscutum constans* and *Watznaueria barnesiae* from the Late Albian “Niveau Breistroffer” (SE France): taxonomic and palaeoecological implications. *Geobios*, 39(5), 599-615. <https://doi.org/10.1016/j.geobios.2005.05.005>
- Bottini, C. and Faucher, G., (2020). *Biscutum constans* coccolith size patterns across the mid Cretaceous in the western Tethys: Paleoecological implications. *Palaeogeography, Palaeoclimatology, Palaeoecology*, 555, 109852. <https://doi.org/10.1016/j.palaeo.2020.109852>
- Bown, P. R. (2005). Calcareous nannoplankton evolution: a tale of two oceans. *Micropaleontology*, 51(4), 299-308. <https://doi.org/10.2113/gsmicropal.51.4.299>
- Bown, P. R., Lees, J. A., and Young, J. R. (2004). Calcareous nannofossil evolution and diversity through time. In Thierstein, H.R., and Young, J.R. (Eds.), *Coccolithophores: From Molecular Process to Global Impact*, Berlin (Springer-Verlag).
- Bown, P.R. and Young, J.R. (1998) Techniques. In: Bown, P.R., Ed., *Calcareous Nannofossil Biostratigraphy* (British micropaleontological Society Publications Series), *Chapman and Kluwer Academic, London*, 16-28.
- Burnett, J. A. (1997). New species and new combinations of Cretaceous nannofossils and a note on the origin of *Petrarhabdus* (Deflandre) Wise and Wind. *Journal of Nannoplankton Research*, 19 (2), 133-146.
- Burnett, J.A. (1998). Upper Cretaceous. In: Bown, P.R. (Ed.), *Calcareous Nannofossil Biostratigraphy*, British Micropaleontology Society Publication Series. Chapman and Hall/Kluwer Academic, London, 132-199.
- Chenot, E., Pellenard, P., Martinez, M., Deconinck, J.F., Amiotte-Suchet, P., Thibault, N., Bruneau, L., Cocquerez, T., Laffont, R., Pucéat, E. and Robaszynski, F. (2016). Clay mineralogical and geochemical expressions of the “Late Campanian Event” in the Aquitaine and Paris basins (France): Palaeoenvironmental implications. *Palaeogeography, Palaeoclimatology, Palaeoecology*, 447, 42-52. <https://doi.org/10.1016/j.palaeo.2016.01.040>

- Chenot, E., Deconinck, J.-F., Pucéat, E., Pellenard, P., Guiraud, M., Jaubert, M., Jarvis, I., Thibault, N., Cocquerez, T., Bruneau, L., Razmjooei, M.J., Boussaha, M., Richard, J., Sizun, J.-P., Stemmerik, L. (2018). Continental weathering as a driver of Late Cretaceous cooling: new insights from clay mineralogy of Campanian sediments from the southern Tethyan margin to the Boreal realm. *Glob. Planet. Chang.* 162, 292-312. <https://doi.org/10.1016/j.gloplacha.2018.01.016>
- Caron, M. (1985). Cretaceous planktic foraminifera. In: Bolli, H.M., Saunders J.B., Perch-Nielsen, K. (Eds.), *Plankton Stratigraphy*. Cambridge University Press, 17-86.
- Clémence, M.E., Gardin, S. and Bartolini, A., (2015). New insights in the pattern and timing of the Early Jurassic calcareous nannofossil crisis. *Palaeogeography, Palaeoclimatology, Palaeoecology*, 427, 100-108. <https://doi.org/10.1016/j.palaeo.2015.03.024>
- Corentin, P., Pucéat, E., Pellenard, P., Freslon, N., Guiraud, M., Blondet, J., Adatte, T. and Bayon, G., (2022). Hafnium-neodymium isotope evidence for enhanced weathering and uplift-climate interactions during the Late Cretaceous. *Chemical Geology*, 591, 120724. <https://doi.org/10.1016/j.chemgeo.2022.120724>
- Deflandre, G. (1959). Sur les nannofossiles calcaires et leur systématique. *Revue de Micropaléontologie*, 2, 127-152.
- Deflandre, G. (1963). Sur les *Microrhabduli*dés, famille nouvelle de nannofossiles calcaires. *Comptes Rendus (Hebdomadaires des Séances) de l'Académie des Sciences Paris*, 256, 3484-3487.
- De Vargas, C., Sáez, A. G., Medlin, L. K. and Thierstein, H. R. (2004). Super-species in the calcareous plankton. In *Coccolithophores*. Springer, Berlin, Heidelberg, 271-298.
- Eppley, R.W., Holmes, R.W. and Strickland, J.D. (1967). Sinking rates of marine phytoplankton measured with a fluorometer. *Journal of experimental marine biology and ecology*, 1(2), 191-208. [https://doi.org/10.1016/0022-0981\(67\)90014-7](https://doi.org/10.1016/0022-0981(67)90014-7)
- Erba, E., Watkins, D. and Mutterlose, J. (1995). Campanian dwarf calcareous nannofossils from Wodejebato Guyot in Haggerty. *Proceedings of the Ocean Drilling Program, Scientific Results*, 144, 141-155. <http://doi.org/10.2973/odp.proc.sr.144.005.1995>
- Faris, M. (1995). Morphometric analysis of *Arkhangelskiella cymbiformis* Vekshina, 1959, in the upper Cretaceous rocks of Egypt and its stratigraphic importance. *Annals of the Geological Survey of Egypt*, 20, 585-601.
- Faucher, G., Visentin, S., Gambacorta, G. and Erba, E. (2022). Schizosphaerella size and abundance variations across the Toarcian Oceanic Anoxic Event in the Sogno Core (Lombardy Basin, Southern Alps). *Palaeogeography, Palaeoclimatology, Palaeoecology*, 595, 110969. <https://doi.org/10.1016/j.palaeo.2022.110969>
- Ferreira, J., Mattioli, E. and van de Schootbrugge, B. (2017). Palaeoenvironmental vs. evolutionary control on size variation of coccoliths across the Lower-Middle Jurassic. *Palaeogeography, Palaeoclimatology, Palaeoecology*, 465, 177-192. <https://doi.org/10.1016/j.palaeo.2016.10.029>
- Gallagher, L.T. (1988). A technique for viewing the same nannofossil specimen in light microscope and scanning electron microscope using standard preparation material. *Journal of Micropaleontology* 7, 53-57.
- Geisen, M., Young, J. R., Probert, I., Sáez, A. G., Baumann, K. H., Sprengel, C., Bollmann, J., Cros, L., De Vargas, C. and Medlin, L. K. (2004). Species level variation in coccolithophores. In *Coccolithophores*. Springer, Berlin, Heidelberg, 327-366.
- Ghiselin, M.T. (1972). Models in phylogeny. In: Schopf, T. J. M., *Models in Paleobiology*. San Francisco: Freeman, Cooper and Company, 130-145.
- Girgis, M. H. (1987). A morphometric analysis of the *Arkhangelskiella* group and its stratigraphical and paleoenvironmental importance. In: Crux, J.A., van Heck, S.E. (Eds.), *Nannofossils and Their Applications*. Ellis Horwood Limited, Chichester (England), 327-339.
- Gollain, B., Mattioli, E., Kenjo, S., Bartolini, A. and Reboulet, S. (2019). Size patterns of the coccolith *Watznaueria barnesiae* in the lower Cretaceous: Biotic versus abiotic forcing. *Marine Micropaleontology*, 152, 101740. <https://doi.org/10.1016/j.marmicro.2019.03.012>
- Gould, S. J. and Eldredge, N. (1977). Punctuated equilibria: the tempo and mode of evolution reconsidered. *Paleobiology*, 3, 115-151. <https://doi.org/10.1017/S0094837300005224>
- Hammer, Ø., Harper, D. A. and Ryan, P. D. (2001). PAST: paleontological statistics software package for education and data analysis. *Paleontologia electronica*, 4(1), 9.

- Hannisdal, B., Henderiks, J. and Liow, L.H. (2012). Long-term evolutionary and ecological responses of calcifying phytoplankton to changes in atmospheric CO<sub>2</sub>. *Global Change Biology*, 18(12), 3504-3516. <https://doi.org/10.1111/gcb.12007>
- Henderiks, J. (2008). Coccolithophore size rules—reconstructing ancient cell geometry and cellular calcite quota from fossil coccoliths. *Marine micropaleontology*, 67(1-2), 143-154. <https://doi.org/10.1016/j.marmicro.2008.01.005>
- Henderiks, J. and Pagani, M. (2008). Coccolithophore cell size and the Paleogene decline in atmospheric CO<sub>2</sub>. *Earth and planetary science letters*, 269(3-4), 576-584. <https://doi.org/10.1016/j.epsl.2008.03.016>
- Henriksson, A. S. and Malmgren, B. A. (1997). Biogeographic and Ecologic Patterns in calcareous nannoplankton in the Atlantic and Pacific Oceans during the Terminal Cretaceous. *Studia Geologica Salmantica*, 33, 17-40.
- Hone, D.W. and Benton, M.J. (2005). The evolution of large size: how does Cope's Rule work?. *Trends in ecology & evolution*, 20(1), 4-6. <https://doi.org/10.1016/j.tree.2004.10.012>
- Huber, B. T. (1990). Maastrichtian planktonic foraminifer biostratigraphy of the Maud Rise (Weddell Sea, Antarctica): ODP Leg 113 Holes 689B and 690C. In: Barker, P.F., Kennett, J.P., Shipboard Scientific Party (Eds.), *Proceedings of the Ocean Drilling Program, Scientific Results*. vol. 113. *Ocean Drilling Program, College Station, TX*, 489-513.
- Huber, B. T. (1992). Upper Cretaceous planktic foraminiferal biozonation for the Austral Realm. *Marine Micropaleontology*, 20, 107-128. [https://doi.org/10.1016/0377-8398\(92\)90002-2](https://doi.org/10.1016/0377-8398(92)90002-2)
- Huber, B.T., Watkins, D.K. (1992). Biogeography of Campanian–Maastrichtian calcareous plankton in the region of the Southern Ocean: paleo-geographic and paleoclimatic implications. In: Kennett, J.P., Warnke, D.A. (Eds.), *The Antarctic Paleoenvironment: a Perspective on Global Change*, vol. 56. *AGU, Antarctic Research Series*, 31-60.
- Hunt, G. and Roy, K. (2006). Climate change, body size evolution, and Cope's Rule in deep-sea ostracodes. *Proceedings of the National Academy of Sciences*, 103(5), 1347-1352. <https://doi.org/10.1073/pnas.0510550103>
- Ifrim, C., Stinnesbeck, W. and López-Oliva, J. G. (2004). Maastrichtian cephalopods from Cerralvo, North-Eastern Mexico. *Paleontology*, 47, 1575-1627. <https://doi.org/10.1111/j.0031-0239.2004.00426.x>
- Ifrim, C., Stinnesbeck, W., Rodríguez Garza, R. and Flores Ventura, J. (2010). Hemipelagic cephalopods from the Maastrichtian (Late Cretaceous) Parras Basin at La Parra, Coahuila, Mexico, and their implications for the correlation of the lower Difunta Group. *Journal of South American Earth Sciences*, 29, 517-618. <https://doi.org/10.1016/j.jsames.2009.08.005>
- Jagt-Yazykova, E. A. (2011). Paleobiogeographical and paleobiological aspects of mid and Late Cretaceous ammonite evolution and bio-events in the Russian Pacific. *Scripta Geologica*, 143, 15-121.
- Jagt-Yazykova, E. A. (2012). Ammonite faunal dynamics across bio-events during the mid- and Late Cretaceous along the Russian Pacific coast. *Acta Paleontologica Polonica*, 57, 737-748. <http://doi.org/10.4202/app.2011.0076>
- Jarvis, I., Gale, A.S., Jenkyns, H.C., Pearce, M.A., (2006). Secular variation in Late Cretaceous carbon isotopes: a new δ<sup>13</sup>C reference curve for the Cenomanian-Campanian (99.6-70.6 Ma). *Geological Magazine* 143, 561-608. <https://doi.org/10.1017/S0016756806002421>
- Johnson, C. C. and Kauffman, E. G. (1996). Maastrichtian extinction patterns of Caribbean province rudistids. In: Macleod, N., Keller, G. (Eds.), *Cretaceous–Tertiary Mass Extinctions: Biotic and Environmental Changes*. W.W. Norton, New York, 231-273.
- Knappertsbusch, M. (2000). Morphologic evolution of the coccolithophorid *C. leptoporus* from the Early Miocene to Recent. *Paleontology*, 74, 712-730. [https://doi.org/10.1666/0022-3360\(2000\)074<0712:MEOTCC>2.0.CO;2](https://doi.org/10.1666/0022-3360(2000)074<0712:MEOTCC>2.0.CO;2)
- Kominz, M.A., Browning, J.V., Miller, K.G., Sugarman, P.J., Mizintseva, S. and Scotese, C.R. (2008). Late Cretaceous to Miocene sea-level estimates from the New Jersey and Delaware coastal plain coreholes: An error analysis. *Basin Research*, 20(2), 211-226. <https://doi.org/10.1111/j.1365-2117.2008.00354.x>
- Lees, J. A. (2002). Calcareous nannofossil biogeography illustrates paleoclimate change in the Late Cretaceous Indian Ocean. *Cretaceous Research*, 23(5), 537-634. <https://doi.org/10.1006/cres.2003.1021>



- Li, L. and Keller, G. (1998). Maastrichtian climate, productivity and faunal turnovers in planktic foraminifera in South Atlantic DSDP sites 525A and 21. *Marine Micropaleontology*, 33(1-2), 55-86. [https://doi.org/10.1016/S0377-8398\(97\)00027-3](https://doi.org/10.1016/S0377-8398(97)00027-3)
- Linnert, C. and Mutterlose, J. (2009). Biometry of the Late Cretaceous *Arkhangelskiella* group: ecophenotypes controlled by nutrient flux. *Cretaceous Research*, 30(5), 1193-1204. <https://doi.org/10.1016/j.cretres.2009.06.001>
- Linnert, C., Mutterlose, J. and Herrle, J. O. (2011). Late Cretaceous (Cenomanian–Maastrichtian) calcareous nannofossils from Goban Spur (DSDP Sites 549, 551): Implications for the paleoceanography of the proto North Atlantic. *Paleogeography, Paleoclimatology, Paleoecology*, 299, 507-528. <https://doi.org/10.1016/j.palaeo.2010.12.001>
- Linnert, C., Mutterlose, J. and Bown, P. R. (2014). Biometry of Upper Cretaceous (Cenomanian–Maastrichtian) coccoliths—a record of long-term stability and interspecies size shifts. *Revue de micropaléontologie*, 57(4), 125-140. <https://doi.org/10.1016/j.revmic.2014.09.001>
- López-Otálvaro, G.E., Suchéras-Marx, B., Giraud, F., Mattioli, E. and Lécuyer, C. (2012). *Discorhabdus* as a key coccolith genus for paleoenvironmental reconstructions (Middle Jurassic, Lusitanian Basin): Biometry and taxonomic status. *Marine Micropaleontology*, 94, 45-57. <https://doi.org/10.1016/j.marmicro.2012.06.003>
- Lübke, N. and Mutterlose, J. (2016). The impact of OAE 1a on marine biota deciphered by size variations of coccoliths. *Cretaceous Research*, 61, 169-179. <https://doi.org/10.1016/j.cretres.2016.01.006>
- Macellari, C. E. (1988). Stratigraphy, sedimentology, and paleoecology of upper Cretaceous/Paleocene shelf deltaic sediments of Seymour Island. In: Feldmann, R.M., Woodburne, M.O. (Eds.), *Geology and Paleontology of Seymour Island, Antarctic Peninsula*. *Geological Society of America*, 169, 25-54.
- Macleod, K. G. (1994). Bioturbation, inoceramid extinction, and mid-Maastrichtian ecological change. *Geology*, 22, 139-142. [https://doi.org/10.1130/0091-7613\(1994\)022<0139:BIEAMM>2.3.CO;2](https://doi.org/10.1130/0091-7613(1994)022<0139:BIEAMM>2.3.CO;2)
- Macleod, K. G. and Ward, P. D. (1990). Extinction pattern of *Inoceramus* (Bivalvia) on shell fragment biostratigraphy. *Geological Society of America Special Papers*, 247, 509-518. <https://doi.org/10.1130/SPE247-p509>
- Marañón, E. (2015). Cell size as a key determinant of phytoplankton metabolism and community structure. *Annual review of marine science*, 241-264. <https://doi.org/10.1146/annurev-marine-010814-015955>
- Meeson, B.W. and Sweeney, B.M. (1982). Adaptation of *Ceratium furca* and *Gonyaulax polyedra* (Dinophyceae) to different temperatures and irradiances: growth rates and cell volumes. *Journal of Phycology* 18, 2, 241-245. <https://doi.org/10.1111/j.1529-8817.1982.tb03180.x>
- Meiri, S. and Dayan, T. (2003). On the validity of Bergmann's rule. *Journal of Biogeography*, 30, 331-351. <https://www.istor.org/stable/3554562>
- Menini, A., Mattioli, E., Hesselbo, S.P., Ruhl, M. and Suan, G. (2021). Primary v. carbonate production in the Toarcian, a case study from the Llanbedr (Mochras Farm) borehole, Wales. *Geological Society, London, Special Publications*, 514(1), 59-81. <https://doi.org/10.1144/SP514-2021-19>
- Miller, K.G., Kominz, M.A., Browning, J.V., Wright, J.D., Mountain, G.S., Katz, M.E., Sugarman, P.J., Cramer, B.S., Christie-Blick, N. and Pekar, S.F., (2005). The Phanerozoic record of global sea-level change. *Science*, 310(5752), 1293-1298. <https://doi.org/10.1126/science.1116412>
- Morgan, K.C. and Kalff, J. (1979). Effect of light and temperature interactions on growth of *Cryptomonas erosa* (Cryptophyceae) 1. *Journal of Phycology*, 15(2), 127-134. <https://doi.org/10.1111/j.1529-8817.1979.tb02975.x>
- Novack-Gottshall, P.M. and Lanier, M.A., 2008. Scale-dependence of Cope's rule in body size evolution of Paleozoic brachiopods. *Proceedings of the National Academy of Sciences*, 105(14), 5430-5434. <https://doi.org/10.1073/pnas.0709645105>
- O'brien, C. L., Robinson, S. A., Pancost, R. D., Damste, J. S. S., Schouten, S., Lunt, D. J., Alsenz, H., Bornemann, A., Bottini, C., Brassell, S. C. and Farnsworth, A. (2017). Cretaceous sea-surface temperature evolution: Constraints from TEX<sub>86</sub> and planktonic foraminiferal oxygen isotopes. *Earth-Science Reviews*, 172, 224-247. <https://doi.org/10.1016/j.earscirev.2017.07.012>
- O'dea, S.A., Gibbs, S.J., Bown, P.R., Young, J.R., Poulton, A.J., Newsam, C. and Wilson, P.A. (2014). Coccolithophore calcification response to past ocean acidification and climate change. *Nature communications*, 5(1), 1-7. <https://doi.org/10.1038/ncomms6363>

- Ovechkina, M. N. and Alekseev, A. S. (2002). Quantitative analysis of Early Campanian calcareous nannofossil assemblages from the southern regions of the Russian Platform. In: M. Wapreith (ed.): Aspects of Cretaceous Stratigraphy and Paleobiostatigraphy. *Österreichische Akademie der Wissenschaften Schriftenreihe der Erdwissenschaftlichen Kommissionen*, 15, 205-221.
- Ovechkina, M. N. and Alekseev A. S. (2005). Quantitative changes of calcareous nannoflora in the Saratov region (Russian Platform) during the late Maastrichtian warming event, *Journal of Iberian Geology*, 31, 149-165.
- Perch-Nielsen, K. (1968). Der Feinbau und die Klassifikation der Coccolithen aus dem Maastrichtien von Dänemark. *Det Kongelige Danske Videnskaberne Selskab Biologiske Skrifter*, 16, 1-96.
- Perch-Nielsen, K. (1973). Neue Coccolithen aus dem Maastrichtien von Danemark, Madagaskar und Ägypten. *Geological Society of Denmark, Bulletin*, 22, 306-333.
- Perch-Nielsen, K. (1985). Mesozoic Calcareous Nannofossils. In: Bolli, H.M., Saunders, J.B., Perch-Nielsen, K. (Eds.), *Plankton Stratigraphy, Cambridge Earth Sciences Series. Cambridge University Press*, 329-426.
- Peti, L. and Thibault, N. (2017). Abundance and size changes in the calcareous nannofossil *Schizosphaerella*—relation to sea-level, the carbonate factory and palaeoenvironmental change from the Sinemurian to earliest Toarcian of the Paris Basin. *Palaeogeography, Palaeoclimatology, Palaeoecology*, 485, 271-282. <https://doi.org/10.1016/j.palaeo.2017.06.019>
- Peti, L., Thibault, N., Korte, C., Ullmann, C.V., Cachão, M. and Fibæk, M. (2021). Environmental drivers of size changes in lower Jurassic *Schizosphaerella* spp. *Marine Micropaleontology*, 168, 102053. <https://doi.org/10.1016/j.marmicro.2021.102053>
- Pirini Radrizzani, C., Castradori, D., Erba, E., Guasti, G. and Rizzi, A. (1990). A revised method for observing the same nannofossils specimens with scanning electron microscope and light microscope. *Rivista Italiana Di Paleontologia* 95, 449-454.
- Piveteau, J. (1952). *Traité de Paléontologie*. In: Grassé, P.P. (Editor), *Traité de zoologie. Anatomie, systématique, biologie*, 1, part 1, Phylogénie. Protozoaires: généralités. Flagellés. *Masson and Cie, Paris*, 107-115.
- Pospichal, J. J. and Wise, S. W. (1990). Calcareous nannofossils across the K–T boundary, ODP-Hole 690 C, Maud Rise, Weddell Sea. *Proceedings of the Oceans Drilling Program, Scientific Results*, 113, 515–532.
- Ratnayake, A.S., Sampei, Y., Ratnayake, N.P. and Roser, B.P. (2017). Middle to late Holocene environmental changes in the depositional system of the tropical brackish Bolgoda Lake, coastal southwest Sri Lanka. *Palaeogeography, Palaeoclimatology, Palaeoecology*, 465, 122-137. <https://doi.org/10.1016/j.palaeo.2016.10.024>
- Razmjooei, M.J., Thibault, N., Kani, A., Mahanipour, A., Boussaha, M., Korte, C. (2014). Coniacian–Maastrichtian calcareous nannofossil biostratigraphy and carbon-isotope stratigraphy in the Zagros Basin (Iran): consequences for the correlation of Late Cretaceous Stage Boundaries between the Tethyan and Boreal realms. *Newsletters on Stratigraphy*, 47(2), 183-209. <https://doi.org/10.1127/0078-0421/2014/0045>
- Razmjooei, M. J., Thibault, N., Kani, A., Dinarès-Turell, J., Pucéat, E., Shahriari, S., Radmacher, W., Jamali, A. M., Ullmann, C. V., Voigt, S. and Cocquerez, T. (2018). Integrated bio-and carbon-isotope stratigraphy of the Upper Cretaceous Gurpi Formation (Iran): a new reference for the eastern Tethys and its implications for large-scale correlation of stage boundaries. *Cretaceous Research*, 91, 312-340. <https://doi.org/10.1016/j.cretres.2018.07.002>
- Razmjooei, M.J., Thibault, N., Kani, A., Ullmann, C.V., Jamali, A.M., (2020a). Santonian-Maastrichtian carbon-isotope stratigraphy and calcareous nannofossil biostratigraphy of the Zagros Basin: Long-range correlation, similarities and differences of carbon-isotope trends at global scale. *Global and Planetary Change*, 184, 103075. <https://doi.org/10.1016/j.gloplacha.2019.103075>
- Razmjooei, M.J., Thibault, N., Kani, A., Dinarès-Turell, J., Pucéat, E., Chin, S., (2020b). Calcareous nannofossil response to Late Cretaceous climate change in the eastern Tethys (Zagros Basin, Iran). *Palaeogeography, Palaeoclimatology, Palaeoecology*, 538, 109418. <https://doi.org/10.1016/j.palaeo.2019.109418>
- Reinhardt, P. (1964). Einige Kalkflagellaten-Gattungen (Coccolithophoriden, Coccolithineen) aus dem Mesozoikum Deutschlands. *Monatsberichte der Deutschen Akademie der Wissenschaften zu Berlin*, 6(10), 749-759.

- Roth, P.H. (1978). Cretaceous nannoplankton biostratigraphy and oceanography of the northwestern Atlantic Ocean. In: In: Benson, W.E., Sheridan, R.E. (Eds.), *Initial Reports of the Deep Sea Drilling Project*, 44, 731-759.
- Roth, P.H. and Krumbach, K.R. (1986). Middle Cretaceous calcareous nannofossil biogeography and preservation in the Atlantic and Indian Oceans: implications for paleoceanography. *Marine Micropaleontology*, 10(1-3), 235-266. [https://doi.org/10.1016/0377-8398\(86\)90031-9](https://doi.org/10.1016/0377-8398(86)90031-9)
- Sáez, A. G., Probert, I., Quinn, P., Young, J. R., Geisen, M. and Medlin, L. K. (2003). Pseudocryptic speciation in coccolithophores. *Proceedings of the National Academy of Sciences*, 100(12), 6893–7418. <https://doi.org/10.1073/pnas.1132069100>
- Schmidt, D.N., Thierstein, H.R., Bollmann, J. and Schiebel, R. (2004). Abiotic forcing of plankton evolution in the Cenozoic. *Science*, 303(5655), 207-210. <https://doi.org/10.1126/science.1090592>
- Schmidt, D.N., Lazarus, D., Young, J.R. and Kucera, M. (2006). Biogeography and evolution of body size in marine plankton. *Earth-Science Reviews*, 78(3-4), 239-266. <https://doi.org/10.1016/j.earscirev.2006.05.004>
- Shamrock, J. L. and Watkins, D. K. (2009). Evolution of the Cretaceous calcareous nannofossil genus *Eiffellithus* and its biostratigraphic significance. *Cretaceous Research*, 30(5), 1083-1102. <https://doi.org/10.1016/j.cretres.2009.03.009>
- Suan, G., Mattioli, E., Pittet, B., Lécuyer, C., Suchéras-Marx, B., Duarte, L.V., Philippe, M., Reggiani, L. and Martineau, F. (2010). Secular environmental precursors to Early Toarcian (Jurassic) extreme climate changes. *Earth and Planetary Science Letters*, 290(3-4), 448-458. <https://doi.org/10.1016/j.epsl.2009.12.047>
- Suchéras-Marx, B., Mattioli, E., Pittet, B., Escarguel, G. and Suan, G. (2010). Astronomically-paced coccolith size variations during the early Pliensbachian (Early Jurassic). *Palaeogeography, Palaeoclimatology, Palaeoecology*, 295(1-2), 281-292. <https://doi.org/10.1016/j.palaeo.2010.06.006>
- Thibault, N. (2010). Biometric analysis of the *Arkhangelskiella* group in the upper Campanian-Maastrichtian of the Stevns-1 borehole, Denmark: taxonomic implications and evolutionary trends. *Geobios*, 43, 639-652. <https://doi.org/10.1016/j.geobios.2010.06.002>
- Thibault, N. (2016). Calcareous nannofossil biostratigraphy and turnover dynamics in the late Campanian–Maastrichtian of the tropical South Atlantic. *Revue de Micropaléontologie*, 59(1), 57-69. <https://doi.org/10.1016/j.revmic.2016.01.001>
- Thibault, N., Minoletti, F., Gardin, S. and Renard, M. (2004). Morphométrie de nannofossiles calcaires au passage Crétacé -Paléocène des coupes de Bidart (France) et d’Elles (Tunisie). Comparaison avec les isotopes stables du carbone et de l’oxygène. *Bulletin de la Societe Geologique de France*, 175, 399-412. <https://doi.org/10.2113/175.4.399>
- Thibault, N., Harlou, R., Schovsbo, N., Schiøler, P., Minoletti, F., Galbrun, B., Lauridsen, B.W., Sheldon, E., Stemmerik, L., Surlyk, F. (2012). Upper Campanian–Maastrichtian nannofossil biostratigraphy and high-resolution carbon-isotope stratigraphy of the Danish Basin: towards a standard  $\delta^{13}C$  curve for the Boreal Realm. *Cretaceous Research*, 33, 72-90. <https://doi.org/10.1016/j.cretres.2011.09.001>
- Thibault, N., Harlou, R., Schovsbo, N. H., Stemmerik, L., Surlyk, F. (2016). Late Cretaceous (Late Campanian–Maastrichtian) sea surface temperature record of the Boreal Chalk Sea. *Climate of the Past*, 12, 1-10. <https://doi.org/10.5194/cp-12-429-2016>
- Thibault, N., Minoletti, F. and Gardin, S. (2018). Offsets in the early Danian recovery phase in carbon isotopes: Evidence from the biometrics and phylogeny of the *Cruciaplacolithus* lineage. *Revue de Micropaléontologie*, 61(3-4), 207-221. <https://doi.org/10.1016/j.revmic.2018.09.002>
- Thierstein, H. R. (1981). Late Cretaceous nannoplankton and the change at the Cretaceous/Tertiary boundary. *Society for Sedimentary Geology Special Publication*, 32, 355-394. <https://doi.org/10.2110/pec.81.32.0355>
- Timofeev, S. F. (2001). Bergmann's principle and deep-water gigantism in marine crustaceans. *Biology Bulletin of the Russian Academy of Sciences*, 28(6), 646-650.
- Varol, O. (1989). Quantitative analysis of the *Arkhangelskiella cymbiformis* group and its biostratigraphical usefulness in the North Sea area. *Journal of Micropaleontology*, 8, 131-134.
- Walsby, A.E. and Reynolds, C.S. (1980). Sinking and floating. In: *The Physiological Ecology of Phytoplankton*, Morris, I.(ed.). 371-412. Blackwell Scientific Publications, Oxford.

- Ward, P. G. (1990). A review of Maastrichtian ammonite ranges. *Geological Society of America Special Papers*, 247, 519-530. <https://doi.org/10.1130/SPE247-p519>
- Ward, P. G., Kennedy, W. J., MacLeod, K. G. and Mount, J. F. (1991). Ammonite and inoceramid bivalve extinction patterns in Cretaceous-Tertiary boundary sections of the Biscay region (southwestern France, Northern Spain). *Geology*, 19, 118-124. [https://doi.org/10.1130/0091-7613\(1991\)019<118:AAIBEP>2.3.CO;2](https://doi.org/10.1130/0091-7613(1991)019<118:AAIBEP>2.3.CO;2)
- Watkins, D.K., (1992). Upper Cretaceous nannofossils from Leg 120, Kerguelen Plateau, Southern Ocean. *Proceedings of the Ocean Drilling Program, Scientific Results 120*, 343-370.
- Wise, S. W. (1983). Mesozoic and Cenozoic calcareous nannofossils recovered by Deep Sea Drilling project Leg 71 in the Falkland Plateau Region, South-west Atlantic Ocean. *Initial Reports of the Deep Sea Drilling Project*, 71, 481-550.
- Wise, S. W. and Wind, F. H. (1977). Mesozoic and Cenozoic calcareous nannofossils recovered by DSDP Leg 36 drilling on the Falkland Plateau, south-west Atlantic sector of the Southern Ocean. *Initial Reports of the Deep Sea Drilling Project*, 36, 269-491.
- Witts, J. D., Bowman, V. C., Wignall, P. B., Crame, J. A., Francis, J. E. and Newton, R. J. (2015). Evolution and extinction of Maastrichtian (Late Cretaceous) cephalopods from the López de Bertodano Formation, Seymour Island, Antarctica. *Paleogeography, Paleoclimatology, Paleoecology*, 418, 193-212. <https://doi.org/10.1016/j.palaeo.2014.11.002>
- Wulff, L., Mutterlose, J. and Bornemann, A., (2020). Size variations and abundance patterns of calcareous nannofossils in mid Barremian black shales of the Boreal Realm (Lower Saxony Basin). *Marine Micropaleontology*, 156, 101853. <https://doi.org/10.1016/j.marmicro.2020.101853>
- Young, J.R., and Bown, P.R. (1997). Higher classification of calcareous nannoplankton. *Journal of Nannoplankton Research* 19, 15-20.
- Young, J.R., Bown, P.R., and Lees J.A., (2017). Nannotax3 website. International Nannoplankton Association. Accessed 21 Apr. 2017. <http://www.mikrotax.org/Nannotax3>